AD_____

Award Number: W81XWH-08-1-0167

TITLE: The Role of Autophagy with Arginine Deiminase as a Novel Prostate Cancer Therapy

PRINCIPAL INVESTIGATOR: Randie Kim

CONTRACTING ORGANIZATION: University of California, Davis
Davis, CA 95616-8671

REPORT DATE: July 2009

TYPE OF REPORT: Annual Summary

PREPARED FOR: U.S. Army Medical Research and Materiel Command
Fort Detrick, Maryland 21702-5012

REPORT DOCUMENTATION PAGE

Form Approved
OMB No. 0704-0188

1. REPORT DATE *(DD-MM-YYYY)*	**2. REPORT TYPE**	**3. DATES COVERED** *(From - To)*
31-07-2009	Annual Summary	1 July 2008 – 30 June 2009

4. TITLE AND SUBTITLE
The Role of Autophagy with Arginine Deiminase as a Novel Prostate Cancer Therapy

5a. CONTRACT NUMBER
W81XWH-08-1-0167

5b. GRANT NUMBER
PC073419

5c. PROGRAM ELEMENT NUMBER

6. AUTHOR(S)
Randie Kim
Email: rhkim@ucdavis.edu

5d. PROJECT NUMBER

5e. TASK NUMBER

5f. WORK UNIT NUMBER

7. PERFORMING ORGANIZATION NAME(S) AND ADDRESS(ES)
University of California, Davis
One Shields Avenue
118 Everson Hall
Davis, CA 95616-8671

8. PERFORMING ORGANIZATION REPORT NUMBER

9. SPONSORING / MONITORING AGENCY NAME(S) AND ADDRESS(ES)
U.S. Army Medical Research and
Material Command
Fort Detrick, Maryland 21702-5012

10. SPONSOR/MONITOR'S ACRONYM(S)

11. SPONSOR/MONITOR'S REPORT NUMBER(S)

12. DISTRIBUTION / AVAILABILITY STATEMENT

Approved for public release; distribution unlimited

13. SUPPLEMENTARY NOTES

14. ABSTRACT

Arginine deprivation by arginine deiminase (ADI) is a novel therapy that is effective against prostate cancers that lack argininosuccinate synthetase (ASS), the rate-limiting enzyme for *de novo* arginine synthesis. We show that in ASS negative CWR22Rv1 prostate cancer cells, ADI rapidly induced autophagy through AMPK/mTOR/S6K as well as ERK1/2 pathways in order to delay the onset of caspase-independent apoptosis. Inhibiting autophagy with chloroquine or Beclin1 siRNA accelerated and enhanced ADI-induced apoptosis. PC3 cells, which express reduced ASS, also undergo autophagy and are responsive to autophagy inhibition and ADI-PEG20 treatment. In contrast, LNCaP cells highly express ASS and are therefore resistant to both ADI-PEG20 and autophagic inhibition. These data point to an interrelationship among ASS deficiency, autophagy, and cell death by ADI-PEG20. Finally, a tissue microarray of 88 prostate tumor samples lacked expression of ASS, indicating ADI-PEG20 is a potential novel therapy for the treatment of prostate cancer.

15. SUBJECT TERMS
prostate cancer; arginine deiminase; autophagy; caspase-independent apoptosis

16. SECURITY CLASSIFICATION OF:			**17. LIMITATION OF ABSTRACT**	**18. NUMBER OF PAGES**	**19a. NAME OF RESPONSIBLE PERSON**
					USAMRMC
a. REPORT	**b. ABSTRACT**	**c. THIS PAGE**			**19b. TELEPHONE NUMBER** *(include area code)*
U	U	U	UU	33	

Table of Contents

Introduction

Arginine deprivation as an anti-cancer therapy has historically been met with limited success. The development of pegylated arginine deiminase (ADI-PEG20) has renewed interest in arginine deprivation for the treatment of some cancers. The efficacy of ADI-PEG20 is directly correlated with argininosuccinate synthetase (ASS) deficiency. Previous *in vitro* studies show the growth of prostate cancer PC3 cells is inhibited when arginine is eliminated from cell culture media (*1*), indicating ADI-PEG20 may be an effective therapy for prostate cancer. Arginine starvation also raises the possibility of the induction of autophagy in response to the metabolic stress. The modulation of autophagy is currently a popular area of research. In particular, the interrelationship between apoptosis and autophagy is significant in cancer development and therapy. Whether autophagy enables cells to survive or die depends on the integration of all inputs to determine a cellular outcome. This project determines the efficacy of ADI-PEG20 on prostate cancer cells, the induction of autophagy by ADI-PEG20, and the modulation of autophagy to enhance the apoptotic effect of ADI-PEG20.

Body

Task 1: To determine the time course of autophagy after ADI-PEG20 treatment in CWR22R*v*1 cells

1a. To detect LC3 cleavage as a marker for autophagy after ADI-PEG20 treatment in CWR22R*v*1 cells.

CWR22R*v*1 cells were treated with 0.3 µg/mL ADI-PEG20 for 0.5, 1, 4, and 24 hours. Expression of LC3-I and its cleavage product LC3-II were examined as a marker for the formation of autophagosomes during autophagy. In addition, autophagic flux was confirmed with the use of a lysosomal inhibitor, chloroquine, leading to the build-up of LC3-II.

Methods: Western blot is described in detail in appended publication (*2*).

Outcomes: LC3-II begins to appear as early as 30 minutes after ADI-PEG20 treatment and persists up to 24 hours (Fig 1a). Co-administration of 25 µM chloroquine confirmed autophagic flux, as evidenced by LC3-II accumulation (Fig 1b). This is described in further detail in Figure 4 in appended publication (*2*).

1b. To analyze cellular acidity as a marker for autophagy after ADI-PEG20 treatment in CWR22R*v*1 cells

CWR22R*v*1 cells were treated with 0.3 µg/mL ADI-PEG20 for 4 and 24 hours. Cellular acidity will be measured using the fluorescent acidotropic dye LysoTracker Green.

Methods: Live cells were trypsinized and resuspended in PBS for live cell analysis by flow cytometry. Cells were incubated with 1, 10, 25, 50, 75 nM LysoTracker Green for

30 minutes or immediately before FACS analysis. Additional detail for flow cytometry is appended (*2*).

Outcomes: By FACS analysis, we were able to plot the signal intensity of the dye vs. the frequency of cells, essentially creating a continuous histogram. However, at 25, 50, and 75 nM LysoTracker Green, the cellular uptake of the dye created a signal distribution that was shifted off scale and thus was unable to be analyzed. At 1 and 10 nM LysoTracker Green, there was no uptake of the dye. Decreasing the incubation time from 30 minutes to immediately prior to FACS analysis had no effect (data not shown).

We therefore attempted to analyze cellular acidity as a proxy for autophagic activity using CWR22R*v*1 cells stably expressing GFP-LC3 protein. According to Shvets and colleagues (*3*), as GFP-LC3 labeled autophagosomes become fused with lysosomes, the acidic environment quenches the GFP signal, which can be detected and measured by flow cytometry. CWR22R*v*1 cells overexpressing GFP-LC3 protein were then treated with 0.3 µg/mL ADI-PEG20 for 4 and 24 hours before FACS analysis.

Methods: Live cells were trypsinized and resuspended in PBS for live cell analysis by flow cytometry. Additional detail for flow cytometry is appended (*2*).

Outcomes: Plotting signal intensity of GFP vs. frequency of cells, we were able to generate a distribution that looks at the global lysosomal activity of a cellular population. However, we were unable to detect the quenching of the GFP signal (indicating increased lysosomal activity and therefore autophagy) under 0.3 µg/mL ADI-PEG20 treatment compared to untreated CWR22R*v*1 cells (data not shown). In addition to 0.3 µg/mL ADI-PEG20, we attempted to validate the method described by Shvets, *et al (3)*, using complete amino acid starvation with HBSS media for 3 and 6 hours as well as 2 µM rapamycin for 24 hours. No appreciable shifts in GFP intensity were detected under these stimuli as well (data not shown).

Task 2: To distinguish between autophagy, autophagic cell death, and apoptotic cell death after ADI treatment in CWR22R*v*1 cells

1a. To evaluate the expression levels of key autophagic proteins after ADI treatment

CWR22Rv1 cells were treated with 0.3 µg/mL ADI for 4, 24, 48, and 96 hours. Total Beclin1 was determined. Beclin1 mRNA was also examined after 96 hours of 0.3 µg/mL ADI-PEG20. The ratio of Beclin1 bound to Bcl-2 by immunoprecipitation was unable to be determined. Protein expression of key autophagy proteins Atg 5, PI3 (III) kinase, UVRAG, Atg 12, and p62 after 0.5, 1, 4, and 24 hours of 0.3 µg/mL ADI-PEG20 was determined. Expression of key autophagy regulators such as phospho-AMP kinase, phospho-mTOR, phospho-S6 kinase, and phospho-S6 protein was also determined after 0.5, 1, 4, and 24 hours of 0.3 µg/mL ADI-PEG20.

Methods: Western blot is described in detail in appended publication (*2*).

Outcomes: While the cleavage of LC3-I into LC3-II after ADI-PEG20 treatment indicates the induction of autophagy, we set out to determine if other proteins in the autophagic pathway are also affected by arginine deprivation. Beclin1 is a critical component of the autophagy pathway; it serves as a scaffold for the recruitment of other autophagy proteins in order to nucleate autophagosomes. Under normal conditions, Beclin1 is bound by Bcl-2 and is released for autophagic induction (*4, 5*). Beclin1 is generally in steady state during autophagy, although some reports have indicated that total Beclin1 may increase under autophagic cell death (*6*).

ADI-PEG20 treatment is able to induce Beclin1 mRNA in CWR22R*v*1 cells after 96 hours (Fig 2a). However, there is no significant increase in Beclin1 protein levels (Fig 2b). Immunoprecipitation of Bcl-2 with subsequent probing of Beclin1 did not reveal any pulldown (data not shown). Immunopreciptation with Beclin1 did pulldown Bcl-2; however, the nonspecific binding of other proteins by the Bcl-2 antibody greatly obscured the Bcl-2 band, making the results inconclusive (data not shown). This suggests that total Bcl-2 is much greater than Beclin1 such that immunopreciptation of Bcl-2 did not bring down enough Beclin1 to be detected on Immunoblot. Therefore, other Bcl-2 antibodies should be tested with Beclin1 immunopreciptation.

Autophagy signaling was also examined by Western. AMP kinase is a sensor for the availability of extracellular nutrients and is directly sensitive to AMP:ATP ratio. Activation of AMP kinase inhibits the mTOR complex via TSC2. The mTOR complex is a key negative regulator of autophagy (*7*). Downstream effectors of mTOR include p70 S6 kinase and S6 protein, which are also implicated in autophagy regulation. The inhibition of mTOR and its subsequent targets leads to the activation of autophagy. Within 30 minutes of 0.3 μg/mL ADI-PEG20, phosphorylation of AMP kinase had increased. Concomitantly, mTOR phosphorylation decreased with subsequent decreases in p70 S6 kinase activity and S6 protein after 24 hours of treatment. (Fig 3a). In addition, ERK1/2 has been known to activated during starvation-induced autophagy (*8, 9*). This signaling pathway is consistent with the activation of autophagy and is described further in Figure 4 of appended publication (*2*).

Other proteins in the autophagy pathway include Atg5, PI3 (Class III) kinase, UVRAG, Atg12, and p62. Protein expression for these components did not change after ADI-PEG20 (Fig 3b). Interestingly, phosphorylation of mTOR downstream effector 4EBP-1 and its target, peIF4E are also unchanged after ADI-PEG20, suggesting that ADI-PEG20 does not signal autophagy through translational regulators (Fig 3b).

1b. To determine if autophagic cell death contributes to tumor cell death after ADI treatment

A tet-inducible Beclin1 or Atg12 knockdown CWR22R*v*1 cell line is necessary to determine the long-term effects of ADI-PEG20 treatment on tumor clonogenicity. Clonogenicity is currently the gold standard for determination of cell death *by* autophagy.

Methods: Attempts to create a CWR22R*v*1 tet-inducible Beclin1 shRNA cell line is described in **Task 3**.

Outcomes: At the conclusion of this project, autophagic cell death (or, cell death *by* autophagy) has not yet been determined after prolonged ADI-PEG20 treatment in CWR22R*v*1 cells. Long-term inhibition of the autophagic pathway (7 days or more) is necessary for colony formation. Transient inhibition through siRNA transfection is not feasible for a clonogenicity experiment. However, long-term chemical inhibition with chloroquine may be an alternative method.

1c. To quantify and distinguish tumor cell death by apoptosis and by autophagy after ADI-PEG20 treatment

CWR22R*v*1 cells were treated with 0.3 µg/mL ADI-PEG20 for 96 hours before analysis with propidium iodide exclusion assay for plasma membrane integrity. Populations were quantified using FACS analysis to plot PI signaling vs. forward-light scattering as a determinant of cell size. During apoptosis, the plasma membrane stays intact while DNA condensation and fragmentation occur. In autophagic cell death, prolonged lysosomal activity disrupts plasma membranes. This gives rise to three populations of cells in which live cells are PI-negative and normal sized, apoptotic cells have low levels of PI staining and smaller sized, and cells undergoing autophagic cell death have high levels of PI staining (*10*).

Methods: CWR22R*v*1 cells were harvested and resuspended in PBS for live cell analysis by FACS. Immediately prior to analysis, propidium iodide stain was added for a final concentration of 0.2 µg/mL. Cells were analyzed by intensity of PI vs. forward-light scattering.

Outcomes: Treatment of CWR22R*v*1 cells with 96 hours of 0.3 µg/mL ADI-PEG20 resulted in a distinct population of live cells that excluded PI stain. However, a distinction between apoptotic cells and autophagic cells was not observed. Cells undergoing death fell within a window of moderate PI staining intensity, with very few cells exhibiting high levels of PI staining. In addition, there was a wide spectrum of cell sizes (data not shown). While it does not exclude the possibility of autophagic cell death, this particular method is not feasible for autophagic cell death quantification.

Task 3: To develop CWR22R*v*1 cell lines with conditional knockdown of autophagic components *Atg12* and/or *Beclin1*.

Development CWR22R*v*1 stably expressing a tet-inducible shRNA against *Beclin1* and *GAPDH* within a lentiviral vector was attempted. TRIPZ lentiviral inducible shRNAmir plasmids (Open Biosystems) contain microRNA-adapted shRNA under tet-inducible promoter, a Turbo-RFP marker for visualizing infection and induction efficiency, and a reverse tet-transactivator for tet-repressor expression.

Methods: 293T cells were seeded in 6-well plates and co-transfected with 0.3 µg

pTRIPZ-shRNA-*Beclin1* and pTRIPZ-shRNA-*GAPDH* (as a positive control) and lentiviral packaging three-plasmid system (0.2 µg pVSV-G, 0.3 µg ΔR8.91) using Transfection reagent (Bio-Rad). Intact viruses shed into the supernatant were collected after 48 hours, clarified at 20,000 x *g* for 5 minutes and stored at -80°C until further use. To transduce cells, CWR22R*v*1 cells were plated in 6-well dishes at a density of 50,000 cells/well to achieve a viral infectivity ratio of at least 10:1. Cells were transduced with 2 mL of lentivirus and 10 µg/mL polybrene at 37°C with 5% CO_2. Supernatant was removed after 4 hours and replaced with fresh RPMI-1640 medium. Selection with 0.5 µg/mL puromycin began 48 hours post-transduction. Cells remained in selection media for one week before harvesting for induction studies. Selected cells were re-seeded and treated with doxycycline for 48 hours. Cells were imaged under fluorescence microscopy to evaluate infection and induction efficacy before harvesting cell lysate for Immunoblot analysis of knockdown.

Outcomes: CWR22R*v*1 cells transduced with pTRIPz-shRNA-*Beclin1* and pTRIPZ-shRNA-*GAPDH* were visualized under fluorescence microscopy after 48 hours of doxycycline. 100% efficiency was determined as all cells expressed TurboRFP under fluorescence microscopy (data not shown). However, immunoblot analysis revealed no knockdown of *Beclin1* and *GAPDH* compared to parental CWR22R*v*1 cells and non-induced CWR22R*v*1 pTRIPz-shRNA-*Beclin1* and CWR22R*v*1 pTRIPz-shRNA-GAPDH (data not shown). Similar results were obtained in transduction of LNCaP cells as well as MiaPaCa2 cells, suggesting that the shRNA from the pTRIPz plasmid is ineffective. Further attempts to create an inducible *Beclin1* knockdown in CWR22R*v*1 have not yet occurred.

Task 4: To evaluate apoptosis after knockdown of autophagy and treatment with ADI-PEG20 in CWR22R*v*1 cells

Inhibition of autophagy in CWR22R*v*1 cells was achieved with chloroquine as well as transient siRNA knockdown of Beclin1. CWR22R*v*1 cells were then treated with 0.3 µg/mL ADI-PEG20 for 24, 48, 72, and 96 hours before FACS analysis of sub-G_1 DNA as a marker for apoptosis.

Methods: Inhibition experiments and FACS analysis are described in detail (*2*).

Outcomes: The inhibition of autophagy by chloroquine or Beclin1 siRNA knockdown accelerated and enhanced the effects of ADI-PE20. In particular, chloroquine led to apoptosis in 30% of CWR22R*v*1 after only 48 hours of ADI-PEG20 treatment (Fig 4a). Beclin1 siRNA provided similar results with an increase in apoptosis after 48 hours of knockdown (Fig 4b, c). These results are described in greater detail in Figure 5 of appended publication (*2*).

Supporting Data

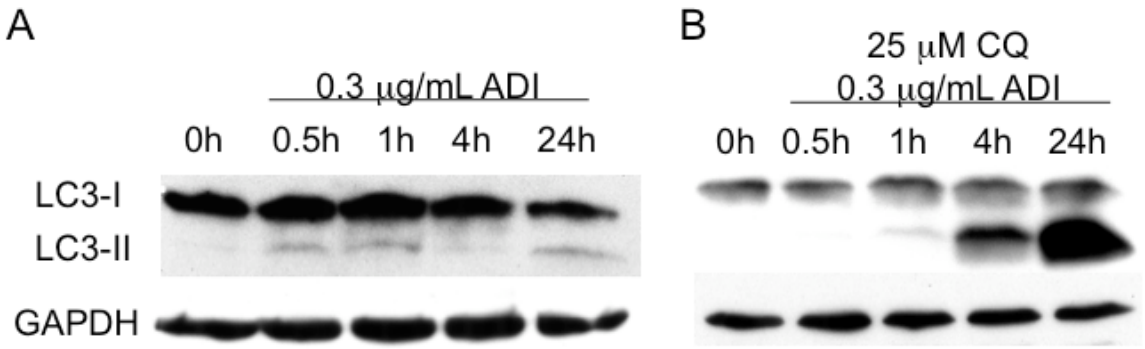

Figure 1. ADI-PEG20 induces autophagy in CWR22R*v*1. *A*, Immunoblot for ADI-PEG20 time course of CWR22R*v*1. CWR22R*v*1 cells overexpressing eGFP-LC3 were treated with 0.3 μg/mL ADI-PEG20 for 0.5, 1, 4, and 24 hours. α-LC3 detects LC3-I and LC3-II. *B*, Autophagic flux was confirmed by co-administering 25 μM chloroquine with 0.3 μg/mL ADI-PEG20 for 0.5, 1, 4, and 24 hours.

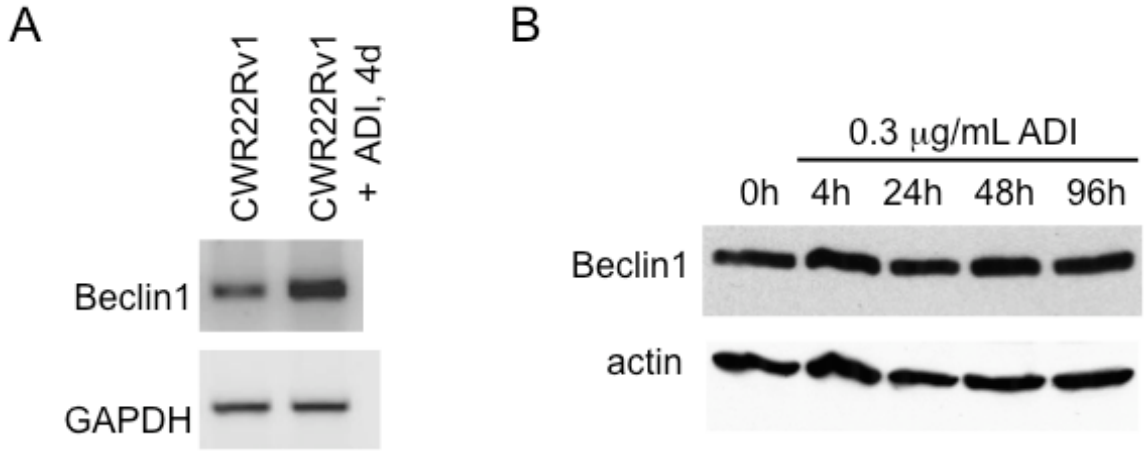

Figure 2. Beclin 1 expression in CWR22R*v*1. *A*, CWR22R*v*1 was examined for Beclin 1 mRNA by RT-PCR. Beclin 1 mRNA expression after 96h of 0.3 μg/mL ADI-PEG20 treatment was also determined. *B*, Immunoblot for 0.3 μg/mL ADI-PEG20 time course in CWR22R*v*1 against α-Beclin 1.

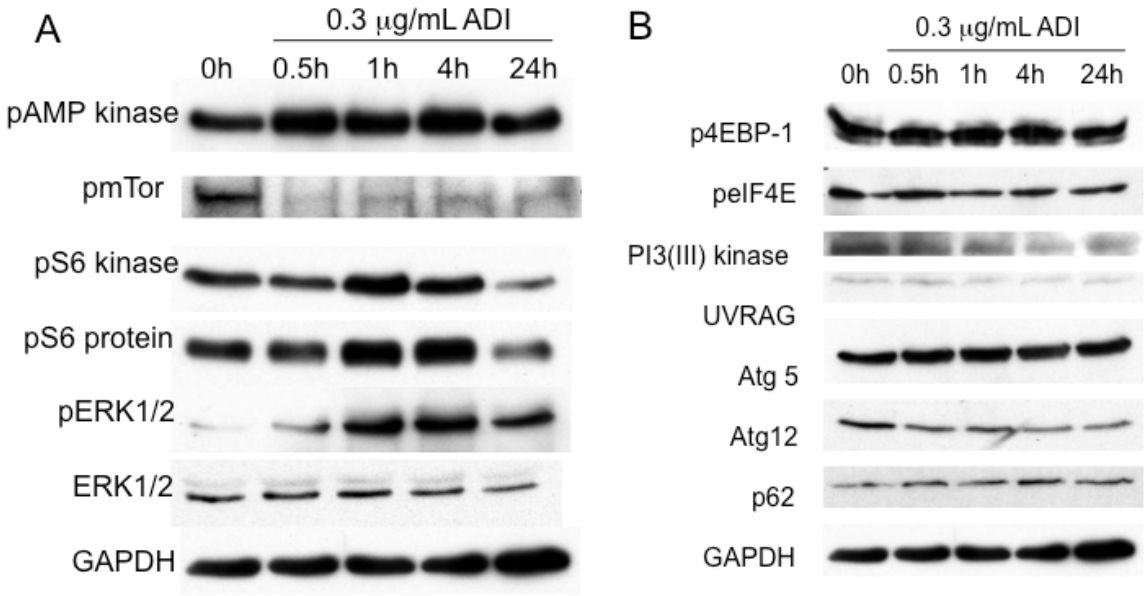

Figure 3. Signaling events and downstream effects after ADI-PEG20 treatment in CWR22R*v*1. *A*, Immunoblot for 0.3 μg/mL ADI-PEG20 time course of CWR22R*v*1 using α-phospho-AMP kinase, α-phospho-mTOR, α-phospho-S6 kinase, α-phospho-S6 protein, α-phospho-ERK1/2, and α-ERK1/2. Loading control for phospho-mTOR was verified using α-tubulin (data not shown). *B*, Immunoblot of downstream mTOR effectors and autophagy proteins after 0.3 μg/mL ADI-PEG20 time course using α-phospho-4EBP-1, α-phospho-eIF4E, α-PI3K (Class III), α-UVRAG, α-Atg5, α-Atg12, and α-p62.

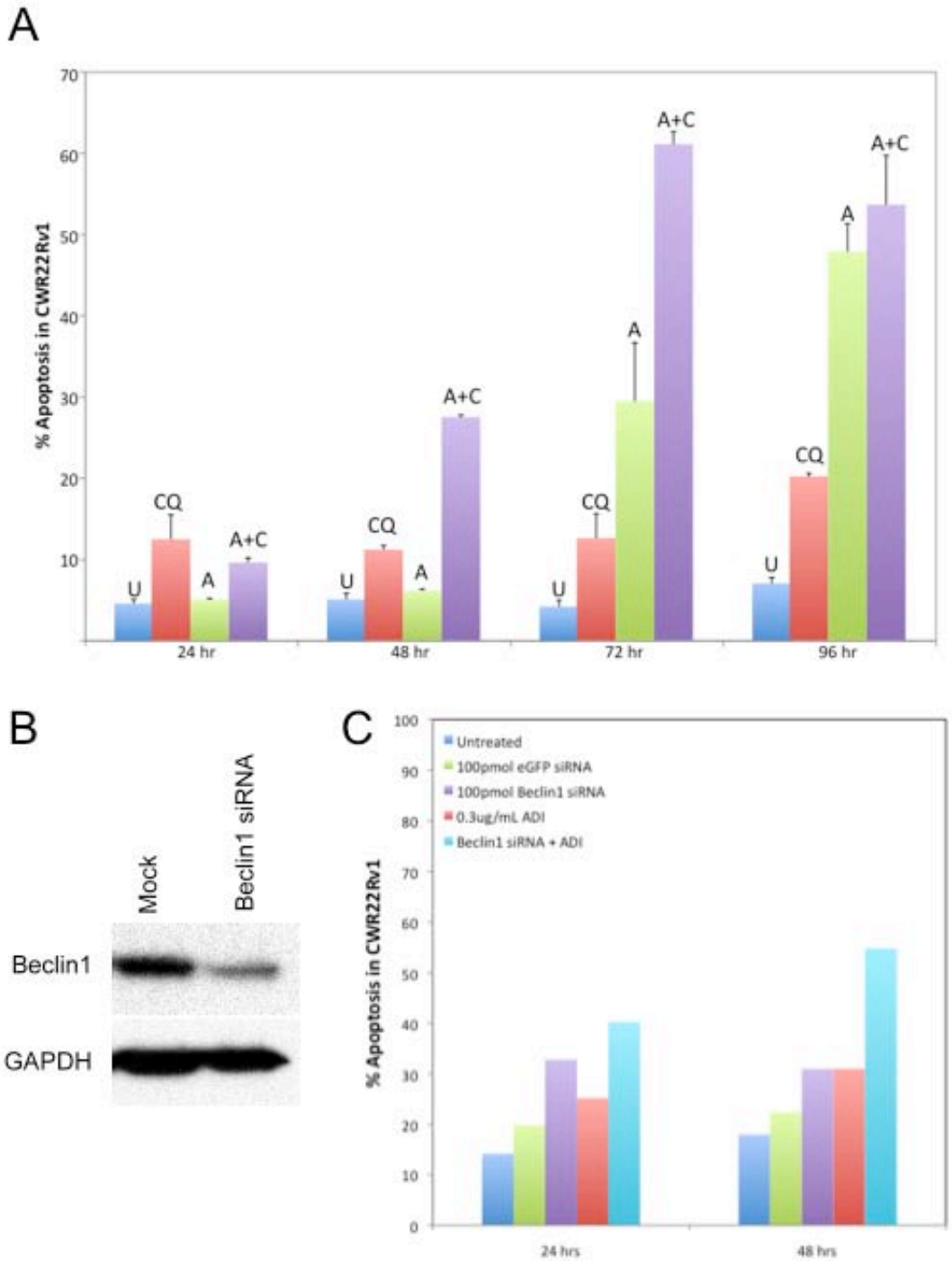

Figure 4. Inhibition of autophagy accelerates and enhances ADI-PEG20-induced cell death. *A*, Time course of CWR22R*v*1 cells treated with vehicle (untreated), 25 μM CQ, 0.1 μg/mL ADI-PEG20, or ADI-PEG20 + CQ before FACS analysis for sub-G_1 content. *Columns*, mean; *bars*, SE. *B*, Immunoblot for CWR22R*v*1 cells transfected with mock or 100 pmol Beclin 1 siRNA to assess knockdown. *C*, CWR22R*v*1 cells were treated with vehicle (untreated), 0.3 μg/mL ADI-PEG20, 100 pmol eGFP siRNA, 100 pmol Beclin 1 siRNA, or Beclin 1 siRNA + ADI-PEG20 for 24 and 48 hours before FACS analysis for sub-G_1 content.

Key Research Accomplishments

- We have demonstrated that ADI-PEG20 is a novel and effective as an anti-cancer agent by inducing caspase-independent apoptosis against ASS negative prostate cancer cell lines *in vitro*.

- We have shown that ADI-PEG20 is effective against CWR22R*v*1 xenografts *in vivo*. By microPET imaging, ADI-PEG20 decreases global tumor metabolic activity within 24 hours. ADI-PEG20 significantly decreases tumor progression in xenografts compared to docetaxel. The combination of docetaxel and ADI-PEG20 is synergistic, arresting tumor progression completely (*2*).

- Using fluorescence microscopy, time-lapsed fluorescence microscopy, and Western blot, we have demonstrated that arginine deprivation by ADI-PEG0 is sufficient to induce autophagy as early as 30 minutes post-treatment.

- We have shown that ADI-PEG20 induces autophagy by signaling through AMPk/mTOR/S6k as well as through the MAPks ERK1/2 (*2*).

- We have demonstrated that autophagy is protective. Inhibition of autophagy enhances and accelerates cell death.

- The absence of ASS expression in prostate cancer is generalizable to human tissue. In a prostate cancer tissue microarray, all 88 tumor samples were not reactive to ASS antibody by immunohistochemistry. Furthermore, ASS mRNA in primary prostate biopsies revealed decreased expression of ASS transcript by RT-PCR (*2*).

Reportable Outcomes

Manuscripts

- Kim RH, Bold RJ, Kung HJ. ADI, autophagy, and apoptosis: Metabolic stress as a therapeutic option for prostate cancer. *Autophagy*. 2009 May 16. Selected for cover image.

- Kim RH, Coates JM, Bowles TL, McNerney GP, Sutcliff J, Jung JU, Gandour-Edwards R, Chuang FY, Bold RJ, Kung HJ. Arginine deiminase as a novel therapy for prostate cancer induces autophagy and caspase-independent apoptosis. *Cancer Res*. 2009 Jan 15; 69(2):700-8. Selected for *Cancer Research Highlights*

Presentations

- Selected to present poster at Autophagy: Cell Biology, Physiology, & Pathology: An EMBO Conference Series; October 18-21, 2009.

Degrees Obtained

- PhD, Biochemistry and Molecular Biology, June 2009 – University of California, Davis

Conclusions

In this report, we showed ADI-PEG20 can effectively induce cell death in prostate cancer cells with low or absent ASS expression. It also sensitizes cells to treatment with docetaxel, an accepted chemotherapy in prostate cancer, or chloroquine, an inhibitor of autophagy. These results are likely to be generally applicable to other prostate cancer cells, since virtually all prostate cancer specimens examined in this report as well as that by Clark and colleagues (*1*) expressed undetectable levels of ASS. By depletion of arginine, ADI-PEG20 causes metabolic stress on auxotrophic cells, complimenting conventional therapies largely based on genotoxic stress. Although arginine deprivation therapy based on bovine arginase has seen limited applications clinically, ADI-PEG20 has 1000-fold greater affinity for arginine (*11*) with fewer side effects. Our work described here thus offers a new treatment option for prostate cancer. In addition, we uncover novel cellular responses of arginine depletion, including autophagy.

The delayed onset of apoptosis suggests the possibility of compensation mechanisms after arginine depletion. Here, we present evidence for the first time that single amino acid starvation through arginine degradation by ADI-PEG20 is sufficient to trigger autophagy in prostate cancer cells. LC3 translocation and cleavage occur within hours of ADI-PEG20 treatment, indicating that autophagy is an early response. AMPK senses cellular AMP/ATP ratio, and in its phosphorylated form, signals the lack of nutrients in the environment to the mTOR complex via TSC2 (*12*). Inhibition of mTOR leads to suppression of S6K activity. Consistent with our findings, Feun and colleagues have reported the effects of ADI-PEG20 on mTOR signaling which include dephosphorylation of mTOR downstream effectors S6K and 4E-BP and increased phosphorylation of AMPK in ASS-negative melanoma cell lines (*13*). This chain of events has been shown to promote autophagy (*14*). There are various signaling cascades that regulate mTOR/S6K including the PI3K (class I)/Akt pathway; inhibition of which has been shown to induce autophagy in malignant gliomas (*8, 15*). While we did not specifically examine the activation of the PI3K (class I)/Akt pathway, ADI-PEG20 inhibited mTOR events associated with a rapid activation of AMPK, suggesting this mechanism in arginine deprivation-induced autophagy. Furthermore, we observed ADI-PEG20 induced ERK1/2 activation, which has been shown to regulate autophagy under a variety of stimuli (*8, 9*).

What is the biological function of ADI-PEG20 induced autophagy? Autophagy can be pro-survival or pro-death, depending on cellular context and duration of treatment. To study whether ADI-PEG20 induced autophagy contributes to or attenuates cell death, we chose to block ADI-PEG20 induced autophagy with the inhibitor chloroquine, which inhibits late stage autophagy by alkalinizing lysosomes and disrupting the autophagolysosome (*16*). Since chloroquine itself may have functions other than inactivating lysosomes (*17*), we also employed siRNA targeting an essential component of autophagy, Beclin 1, a component of the class III PI3 kinase complex that nucleates autophagosomes (*18*). Our data show inhibition of early stage autophagy by chloroquine or Beclin 1 knockdown accelerates and enhances cell death after ADI-PEG20, strongly suggesting ADI-PEG20 induced autophagy triggers a protective

response during early stages of treatment. At present, we cannot rule out that prolonged ADI-PEG20 treatment (>96 hours) may trigger autophagic cell death (programmed cell death type II), which is usually caspase-independent. In our study, we found chloroquine itself had little effect on the cell killing of CWR22R*v*1, unless ADI-PEG20 is present and autophagy is induced. In addition, co-administration of chloroquine with ADI-PEG20 did not activate caspase-3. This again suggests that the major effect of chloroquine is to block autophagy, enhancing the underlying mechanism of caspase-independent apoptosis. Consistent with this result, PC3 cells with reduced ASS levels also underwent autophagy after ADI-PEG20 treatment. The inhibition of autophagy with 3-MA significantly reduced cell proliferation in the presence of ADI-PEG20. Both chloroquine and ADI-PEG20 have no effect on LNCaP cells, which express ASS. Interestingly, ASS-positive hepatocellular carcinomas resistant to ADI-PEG20 responded to arginine deprivation by pegylated recombinant arginase (*19*), providing a potential alternative to ADI-PEG20-resistant tumors and cell lines such as LNCaP.

In cancer, an autophagy paradox has emerged in which survival and death are context specific, particularly due to complex interactions between autophagic and apoptotic pathways. Accordingly, cancer therapies have been reported to have opposing effects on cell death. Photodynamic therapy promotes autophagic cell death in apoptosis-deficient cancer cells (*20*) while sulforaphane-induced autophagy in PC3 and LNCaP is protective (*21*). Furthermore, manipulation of autophagy can sensitize tumor cells to subsequent treatments. Induction of autophagy by an mTOR inhibitor increased prostate cancer cell susceptibility to irradiation (*22*). Conversely, chloroquine is a highly promising autophagy inhibitor for clinical use. Although it is extensively used to treat malaria (*23*), its uses against cancer are only recently emerging. In a *myc*-induced lymphoma model, autophagic inhibition by chloroquine enhanced the ability of alkylating agents to suppress tumor growth (*24*). This underscores the importance of autophagy to fundamental cell processes and its ability to modulate the effect of chemotherapies across a wide variety of cancers.

The absence of ASS as a biomarker for ADI-PEG20 efficacy has previously been established in hepatoma and melanoma cell lines. Phase I/II clinical trials with ADI-PEG20 led to a 47% response rate in patients with unresectable hepatocellular carcinomas and a 25% response rate in metastatic melanoma patients (*25, 26*). In this study, we show ADI-PEG20 can be effective against prostate cancer. ASS expression can be determined by immunohistochemistry and potentially be used as a clinical indicator for ADI-PEG20 use. The absence of ASS protein in all examined prostate tumor samples makes ADI-PEG20 a promising therapeutic avenue to follow. The combination of ADI-PEG20, which induces caspase-independent apoptosis, and taxanes, which are caspase-dependent, is more effective than monotherapy. This concept of synergistic interaction between cancer therapies is an active area of research. In particular, combining therapies that target different mechanisms of cell death may increase efficacy beyond either agent alone. Furthermore, the rise of advanced imaging for tumor assessment and staging may allow clinical monitoring of tumor responsiveness to ADI-PEG20 by PET. Finally, arginine deprivation by ADI-PEG20 induces autophagy as a protective mechanism. Co-administration with an

autophagic inhibitor such as chloroquine can potentially enhance cell death in prostate tumors. The intricate link between autophagy and apoptosis points to autophagy as an additional target for anti-cancer treatments. Thus, ADI-PEG20 is a novel prostate cancer therapy whose mechanism of action can be complemented by other chemotherapies to maximize cell death.

References

1. B. J. Dillon *et al.*, *Cancer* **100**, 826 (Feb 15, 2004).
2. R. H. Kim *et al.*, *Cancer Res* **69**, 700 (Jan 15, 2009).
3. E. Shvets, E. Fass, Z. Elazar, *Autophagy* **4**, 621 (Jul 1, 2008).
4. M. C. Maiuri *et al.*, *EMBO J* **26**, 2527 (May 16, 2007).
5. A. Oberstein, P. D. Jeffrey, Y. Shi, *J Biol Chem* **282**, 13123 (Apr 27, 2007).
6. S. Pattingre, B. Levine, *Cancer Res* **66**, 2885 (Mar 15, 2006).
7. S. Pattingre, L. Espert, M. Biard-Piechaczyk, P. Codogno, *Biochimie* **90**, 313 (Feb, 2008).
8. N. Shinojima, T. Yokoyama, Y. Kondo, S. Kondo, *Autophagy* **3**, 635 (Nov-Dec, 2007).
9. S. Pattingre, C. Bauvy, P. Codogno, *J Biol Chem* **278**, 16667 (May 9, 2003).
10. K. Ono, S. O. Kim, J. Han, *Mol Cell Biol* **23**, 665 (Jan, 2003).
11. B. J. Dillon, F. W. Holtsberg, C. M. Ensor, J. S. Bomalaski, M. A. Clark, *Med Sci Monit* **8**, BR248 (Jul, 2002).
12. D. G. Hardie, *J Cell Sci* **117**, 5479 (Nov 1, 2004).
13. L. Feun *et al.*, *Curr Pharm Des* **14**, 1049 (2008).
14. Z. X. Xu *et al.*, *Cell Death Differ* **14**, 1948 (Nov, 2007).
15. H. Aoki *et al.*, *Mol Pharmacol* **72**, 29 (Jul, 2007).
16. M. C. Maiuri, E. Zalckvar, A. Kimchi, G. Kroemer, *Nat Rev Mol Cell Biol* **8**, 741 (Sep, 2007).
17. K. H. Maclean, F. C. Dorsey, J. L. Cleveland, M. B. Kastan, *J Clin Invest* **118**, 79 (Jan, 2008).
18. C. Liang *et al.*, *Nat Cell Biol* **10**, 776 (Jul, 2008).
19. P. N. Cheng *et al.*, *Cancer Res* **67**, 309 (Jan 1, 2007).
20. L. Y. Xue, S. M. Chiu, K. Azizuddin, S. Joseph, N. L. Oleinick, *Autophagy* **4**, 125 (Jan 1, 2008).
21. A. Herman-Antosiewicz, D. E. Johnson, S. V. Singh, *Cancer Res* **66**, 5828 (Jun 1, 2006).
22. C. Cao *et al.*, *Cancer Res* **66**, 10040 (Oct 15, 2006).
23. R. K. Amaravadi, C. B. Thompson, *Clin Cancer Res* **13**, 7271 (Dec 15, 2007).
24. R. K. Amaravadi *et al.*, *J Clin Invest* **117**, 326 (Feb, 2007).
25. F. Izzo *et al.*, *J Clin Oncol* **22**, 1815 (May 15, 2004).
26. P. A. Ascierto *et al.*, *J Clin Oncol* **23**, 7660 (Oct 20, 2005).

Appendices

- Curriculum Vitae

- Abstract for poster presentation at at Autophagy: Cell Biology, Physiology, & Pathology: An EMBO Conference Series; October 18-21, 2009, Ascona, Switzerland.

- Kim RH, Coates JM, Bowles TL, McNerney GP, Sutcliff J, Jung JU, Gandour-Edwards R, Chuang FY, Bold RJ, Kung HJ. Arginine deiminase as a novel therapy for prostate cancer induces autophagy and caspase-independent apoptosis. *Cancer Res*. 2009 Jan 15; 69(2):700-8.

- Kim RH, Bold RJ, Kung HJ. ADI, autophagy, and apoptosis: Metabolic stress as a therapeutic option for prostate cancer. *Autophagy*. 2009 May 16.

Abstract

Autophagy: Cell Biology, Physiology, & Pathology: An EMBO Conference Series
October 18-21, 2009, Ascona, Switzerland

Arginine deprivation by arginine deiminase (ADI) is a novel therapy that is effective against prostate cancers that lack argininosuccinate synthetase (ASS), the rate-limiting enzyme for *de novo* arginine synthesis. We have previously shown that in ASS negative CWR22R*v*1 prostate cancer cells, ADI rapidly induces autophagy through AMPK/mTOR/S6K as well as ERK1/2 pathways in order to delay the onset of caspase-independent apoptosis. Inhibiting autophagy with chloroquine or Beclin1 siRNA accelerates and enhances ADI-induced apoptosis. In addition, we hope to use ADI as a tool to develop a quantitative image cytometry assay for autophagy. CWR22R*v*1 cells overexpressing eGFP-LC3, RFP-LAMP1, and stained with Hoechst live cell nuclear stain were treated with ADI and imaged over time. Autophagosome formation was readily induced by ADI and co-localization with lysosomes appeared to increase over time, confirming autophagic flux. Apoptosis was detected after 72 hours of ADI treatment although autophagy in these cells was greatly diminished. Using Volocity, a high performance 3D imaging software, parameters such as autophagosome size, fluorescent intensity, kinetics, half-life, and degree of co-localization with lysosomes can potentially be extracted from 3D and 4D images. Additional fluorescent labels in conjunction with image cytometry can therefore provide direct measurements from which mechanistic inferences can be made, providing a novel and powerful tool to the field of autophagy.

Arginine Deiminase as a Novel Therapy for Prostate Cancer Induces Autophagy and Caspase-Independent Apoptosis

Randie H. Kim,[1] Jodi M. Coates,[2] Tawnya L. Bowles,[2] Gregory P. McNerney,[3] Julie Sutcliffe,[4] Jae U. Jung,[6] Regina Gandour-Edwards,[5] Frank Y.S. Chuang,[3] Richard J. Bold,[2] and Hsing-Jien Kung[1]

Departments of [1]Biological Chemistry, [2]Surgery (Division of Surgical Oncology), [3]Biophysics (Center for Biophotonics and Science Technology), [4]Biomedical Engineering, and [5]Pathology, University of California at Davis, Sacramento, California; and [6]Department of Molecular Microbiology and Immunology, University of Southern California Keck Medical School, Los Angeles, California

Abstract

Arginine deprivation as an anticancer therapy has historically been met with limited success. The development of pegylated arginine deiminase (ADI-PEG20) has renewed interest in arginine deprivation for the treatment of some cancers. The efficacy of ADI-PEG20 is directly correlated with argininosuccinate synthetase (ASS) deficiency. CWR22R*v*1 prostate cancer cells do not express ASS, the rate-limiting enzyme in arginine synthesis, and are susceptible to ADI-PEG20 *in vitro*. Interestingly, apoptosis by 0.3 μg/mL ADI-PEG20 occurs 96 hours posttreatment and is caspase independent. The effect of ADI-PEG20 *in vivo* reveals reduced tumor activity by micropositron emission tomography as well as reduced tumor growth as a monotherapy and in combination with docetaxel against CWR22R*v*1 mouse xenografts. In addition, we show autophagy is induced by single amino acid depletion by ADI-PEG20. Here, autophagy is an early event that is detected within 1 to 4 hours of 0.3 μg/mL ADI-PEG20 treatment and is an initial protective response to ADI-PEG20 in CWR22R*v*1 cells. Significantly, the inhibition of autophagy by chloroquine and Beclin1 siRNA knockdown enhances and accelerates ADI-PEG20–induced cell death. PC3 cells, which express reduced ASS, also undergo autophagy and are responsive to autophagy inhibition and ADI-PEG20 treatment. In contrast, LNCaP cells highly express ASS and are therefore resistant to both ADI-PEG20 and autophagic inhibition. These data point to an interrelationship among ASS deficiency, autophagy, and cell death by ADI-PEG20. Finally, a tissue microarray of 88 prostate tumor samples lacked expression of ASS, indicating ADI-PEG20 is a potential novel therapy for the treatment of prostate cancer. [Cancer Res 2009;69(2):700–8]

Introduction

The initial observations that various tumor cells are susceptible to arginine deprivation were made over 40 years ago, although appropriate therapeutic methods have hindered further development of this approach until recently. Arginine deiminase (ADI), an enzyme isolated from *Mycoplasma* (1, 2), degrades arginine into its citrulline precursor. In its native form, it is strongly antigenic with a half-life of 5 hours (3). Conjugation to 20,000 mw polyethylene glycol (ADI-PEG20) decreases antigenicity as well as dramatically increases serum half-life, allowing weekly administration that reduces plasma arginine to undetectable levels (4, 5). Various tumor types (hepatocellular carcinomas, melanomas, mesotheliomas, renal cell carcinomas, pancreatic carcinomas) have been shown to lack expression of argininosuccinate synthetase (ASS; refs. 4, 6–8), a ubiquitous enzyme involved in the two-step synthesis of arginine from citrulline (9). Unable to synthesize their own arginine, ASS-deficient cells depend on relatively inefficient amino acid transporters (10). In the setting of ASS deficiency, ADI-PEG20 depletes intracellular arginine by reducing extracellular levels available for transmembrane uptake while unaffecting cells with preserved ASS expression capable of endogenous arginine biosynthesis (11). Previous *in vitro* studies show the growth of prostate cancer PC3 cells is inhibited when arginine is eliminated from cell culture medium (12), indicating ADI-PEG20 may be an effective therapy for prostate cancers.

The antitumor effects of ADI-PEG20 elicit a G_1 cell cycle arrest with eventual apoptosis in a number of tumor cell lines (13). In addition, ADI-PEG20 is antiangiogenic, inhibiting migration and tube formation in HUVE cells (14) and neovascularization of neuroblastomas *in vivo* (15). However, other cellular effects of arginine starvation by ADI-PEG20 are still unknown.

Nutrient depletion triggers a process called macroautophagy (hereafter called autophagy), an evolutionary conserved eukaryotic process in which organelles and bulk proteins are turned over by lysosomal activity. Autophagy serves to provide ATP and other macromolecules as energy sources during metabolic stress (16, 17). The most distinctive feature of autophagy is the formation of the autophagosome, a double-membrane vesicle that fuses with lysosomes for hydrolytic cleavage of engulfed proteins and organelles. In mammalian cells, microtubule-associated protein 1 light chain 3 (LC3) is processed by lipid conjugation to phosphatidylethanolamine for insertion into the autophagosome membrane (18). Translocation and processing of an eGFP-LC3 fusion protein are often used as markers for autophagic activity.

Autophagy has recently gained much attention for its paradoxical roles in cell survival and cell death, particularly in the pathogenesis as well as the treatment of cancer (19, 20). Regulation of autophagy is highly complex with inputs from the cellular environment through the phosphatidylinositol-3-OH kinase (PI3K)/Akt/mammalian target of rapamycin (mTOR) pathway (21), members of the Bcl2 family (22), p53 (23), and death-associated protein kinases (24). Not surprisingly, there is an intricate relationship between autophagy and apoptosis. Whether autophagy enables cells to survive or enhances their death is context-driven, depending on the type of stimuli, nutrient availability, organism

Requests for reprints: Hsing-Jien Kung, UC Davis Cancer Center, University of California - Davis Medical Center, Research III, Room 2400B, 4645 2nd Avenue, Sacramento, CA 95817. Phone: 916-734-1538; Fax: 916-734-2589; E-mail: hkung@ucdavis.edu and Richard J. Bold, University of California - Davis Medical Center, 4501 X Street, Sacramento, CA 95817. Phone: 916-734-5907; Fax: 916-703-5267; E-mail: richard.bold@ucdmc.ucdavis.edu.

doi:10.1158/0008-5472.CAN-08-3157

development, and apoptotic status. We hypothesize prostate cancer cells that are ASS deficient are sensitive to arginine deprivation by ADI-PEG20 and consequently, undergo autophagy as an initial survival response.

In this study, we show susceptibility of several prostate cancer cell lines to ADI-PEG20 correlates with the absence of ASS expression. Due to the lack of ASS, ADI-PEG20 induces a late caspase-independent cell death in CWR22Rv1 *in vitro*. Metabolic activity by micro positron emission tomography (microPET) imaging of CWR22Rv1 xenografts in nude mice was reduced by ADI-PEG20. Tumor growth was significantly inhibited by ADI-PEG20 alone as well as in combination with docetaxel. ADI-PEG20 also induces autophagy within hours of treatment. However, inhibition of autophagy prematurely leads to cell death by ADI-PEG20. With the success of ADI-PEG20 therapy for hepatocellular carcinomas and melanomas and our findings that prostate cancer specimens lack ASS expression, ADI-PEG20 can potentially be extended to clinical trials for prostate cancer. Moreover, combination with standard chemotherapies or autophagy-targeting drugs represents multipronged approaches to cancer therapy.

Materials and methods

Reagents. Recombinant ADI formulated with multiple linear 20,000 mw polyethylene glycol molecules (ADI-PEG20) was generously provided by DesigneRx Pharmaceuticals, Inc. Specific enzyme activity was 7.4 IU/mg. Internal calibration of enzyme IC_{50} was determined with each batch.

Cells and cell culture. All cell lines were cultured in RPMI 1640 [10% fetal bovine serum (FBS), 1% penicillin, streptomycin, glutamine]. LNCaP cells were cultured in serum-free, phenol-free medium before 10 nmol/L 5α-Dihydrotestosterone (DHT; Sigma) treatment for 4, 24, and 48 h. PC3 cells were transiently transfected and CWR22Rv1 cells were stably transfected with eGFP-LC3 plasmid (JUJ) using Effectene (Qiagen).

Reverse transcription-PCR and quantitative reverse transcription-PCR. Total RNA was isolated from cultured cells by TRIzol (Invitrogen) homogenization and reverse transcribed using Moloney murine leukemia virus (Invitrogen). One hundred nanograms of cDNA were PCR amplified as described previously (25). Primers: ASS (F) 5′-GACGCTATGTCCAGCAAAG-3′ and (R) 5′-TTGCTTTGCGTACTCCATCAG-3′; glyceraldehyde-3-phosphate dehydrogenase (GAPDH; F) 5′-ACCACAGTCCATGCCATCAC-3′ and (R) 5′-TCCACCACCCTGTTGCTGTA-3′. Total RNA from primary prostate tissues was reverse transcribed using SuperScriptIII (Invitrogen). One hundred nanograms of cDNA were amplified by iQ5 iCycler thermal cycler (Bio-Rad) and monitored by SYBRGreen (Invitrogen) for real-time PCR. Threshold cycle values were normalized against actin and analyzed using QGene software. Primers were as follows: ASS (F) 5′-TGAAATTTGCTGAGCTGGTG-3′ and (R) 5′-ATGTACACCTGGCCCTTGAG-3′; Actin (F) 5′-TCCTTAATGTCACGCACGATTT-3′ and (R) 5′-GAGCGCGGCTACAGCTT-3′.

Immunoblotting. Cellular lysates were resolved on SDS-PAGE and electrophoretically transferred to polyvinylidene difluoride membranes. Membranes were incubated with primary antibody followed by species-specific horseradish peroxidase secondary antibody. Immunoreactive material was detected by chemiluminescence (Pierce Laboratories). Antibodies were as follows: actin (Santa Cruz Biotechnology), ASS (BD Biosciences), caspase-3 (Biosource), GAPDH (Chemicon), tubulin (Sigma), Beclin1, phospho-AMP kinase (Thr172), phospho-mTor (Ser2481), phospho-S6 kinase (Thr389), phospho-S6 (Ser235/236), LC3, extracellular signal-regulated kinase (ERK)1/2, and phospho-ERK1/2 (Cell Signaling).

3-(4,5-Dimethylthiazol-2-yl)-2,5-diphenyltetrazolium bromide cytotoxicity assay. RWPE-1, LNCaP, PC3, and CWR22Rv1 cells were seeded in 96-well plates and treated with serial dilutions of ADI-PEG20. After 6 d, thiazolyl blue tetrazolium bromide (MTT; Sigma) was added for a final concentration of 0.5 mg/mL. PC3 cells were treated for 3 d in 2% FBS. Formazan crystals were solubilized by 10% SDS. The IC_{50} is the drug concentration at which 50% of cell growth is inhibited.

Fluorescence-activated cell sorting analysis for sub-G_1 DNA fragmentation. CWR22Rv1 cells were treated with 0.3 μg/mL ADI-PEG20, 100 nmol/L paclitaxel (Sigma), or pretreated with 50 μmol/L z-VAD-fmk (MBL International). Cells were analyzed by flow cytometry as described previously (8).

Active caspase-3 ELISA. CWR22Rv1 cells were seeded in 6-well plates and treated with 100 nmol/L paclitaxel or 0.3 μg/mL ADI-PEG20 for 24 h. Treatment groups were compared with cells pretreated with 50 μmol/L z-VAD-fmk for 2 h before assaying for activated caspase-3 by ELISA (R&D Systems).

MicroPET imaging. Nude mice with CWR22Rv1 s.c. xenografts were injected via tail vein with 120 mCi of ^{18}F-FDG and imaged by PET as described previously (26) before and after 5 IU ADI-PEG20 treatment of 4 or 24 h. Standard uptake values (SUV) were computed by dividing the activity concentration in each voxel by the injected dose and multiplying by animal weight. Absolute uptake values of posttreatment images were normalized to pretreatment images before analysis.

Xenograft efficacy studies. For tumorigenesis, 1×10^6 CWR22Rv1 cells were injected s.c. into the bilateral flanks of male athymic BALB/c mice (Harlan Sprague-Dawley, Inc). Mice received weekly 0.5 mL i.p. injections of sterile PBS (n = 4), 10 mg/kg docetaxel (n = 4), 5 IU (225 μg/mL) ADI-PEG20 (n = 4), or both 10 mg/kg docetaxel and 5 IU ADI-PEG20 (1 mL total volume; n = 4). Tumor dimensions were measured twice weekly. Tumor volumes were calculated by $V = 0.5236\ (L \times W^2)$, L = length, W = width.

Fluorescence microscopy for LC3. CWR22Rv1 and PC3 cells overexpressing eGFP-LC3 were seeded on poly-lysine–coated coverslips. Cells were treated with 0.3 μg/mL ADI-PEG20 for 4 or 24 h or 2 μmol/L rapamycin for 4 h. Cells were fixed, mounted using SlowFade with 4′,6-diamidino-2-phenylindole (DAPI; Invitrogen), and examined under a ×60 lens on an Olympus BX61 motorized reflected fluorescence microscope with an AMCA filter (excitation, 350 nm; emission, 460 nm) for DAPI and FITC filter (excitation, 480 nm; emission, 535 nm) for eGFP-LC3 using SlideBook4.1 software (Intelligent Imaging Innovations).

For live cell imaging, CWR22Rv1 cells overexpressing eGFP-LC3 were plated on 35 mm #1 glass bottom dishes (WillCo Wells), treated with 0.3 μg/mL ADI-PEG20, and imaged with an IX-71 inverted microscope with a ×100 1.40 NA oil objective (Olympus) and ASI 400 air stream incubator (NEVTEK) set to 37°C. Images were acquired using a spinning disc system.

Inhibition of autophagy. CWR22Rv1 cells were treated with 25 μmol/L chloroquine (Sigma), 0.1 μg/mL ADI-PEG20, or both for 24, 48, 72, and 96 h. LNCaP cells were treated as above except with 0.3 μg/mL ADI-PEG20. Cells were analyzed by fluorescence-activated cell sorting (FACS) analysis as described previously.

CWR22Rv1 cells were seeded in 6-well plates then transiently transfected with 100 pmol eGFP siRNA (Ambion) or Beclin1 siRNA ON-TARGETplus SMARTpool (Dharmacon) using DharmaFECT

reagent (Dharmacon). Cells were treated with 0.3 μg/mL ADI-PEG20 for 24 or 48 h the following day and analyzed by FACS analysis as described previously.

PC3 cells were treated with 0.3 μg/mL ADI-PEG20, 5 μg/mL ADI-PEG20, 1 mmol/L 3-methyladenine (3-MA; Sigma), or both for 24, 48, and 72 h and analyzed by MTT as described previously.

ASS immunohistochemistry. Formalin-fixed, paraffin-embedded archival material from 88 prostate tumors and 59 normal prostate samples were obtained. Tumors represent a range of Gleason grades (3+3 = 6 to 4+5 = 9). H&E-stained sections were made from each block to define representative tumor regions, and a tumor microarray (TMA) was constructed. TMA paraffin blocks were sectioned at 4 μm and transferred to glass slides. Immunohistochemistry was performed using α-ASS monoclonal mouse antibody (DesigneRx Pharmacologies) at 2.2 μg/mL. Normal liver was used as a positive control. Omission of primary antibody was used as negative control. Sections were counterstained with Gill's hematoxylin and fixed. Slides were independently examined by a board certified anatomic pathologist (RGE) thrice and scored by percentage of cells stained.

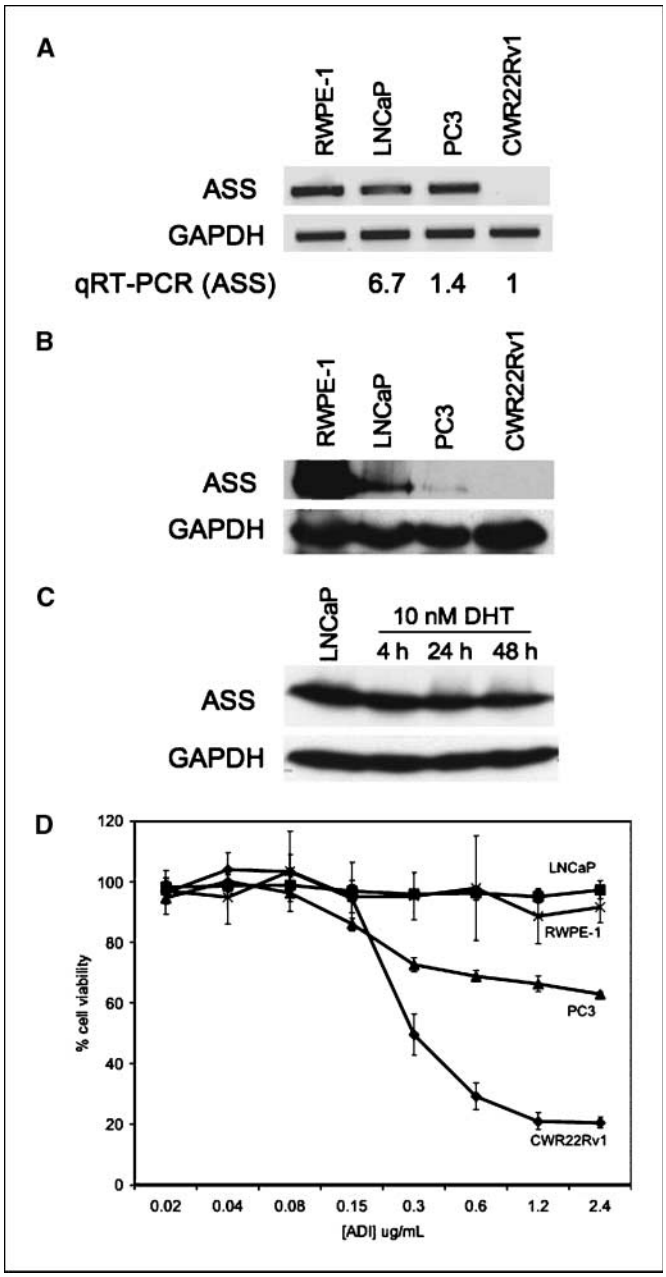

Figure 1. Prostate cancer cell lines profiled for ASS expression and ADI-PEG20 sensitivity. RWPE-1, LNCaP, PC3, and CWR22Rv1 were examined for ASS mRNA by RT-PCR (*A*) and ASS protein by immunoblotting (*B*). *C,* immunoblot for 10 nmol/L DHT time course of LNCaP against α-ASS. *D,* cell lines were treated by ADI-PEG20 at 0.02, 0.04, 0.08, 0.15, 0.3, 0.6, 1.2, and 2.4 μg/mL for 3 (PC3) or 6 d before MTT assay. *Points,* mean; *bars,* SD.

Results

Sensitivity to ADI-PEG20 correlates with ASS expression. ASS expression in three commonly cultured prostate carcinoma cell lines (LNCaP, PC3, CWR22Rν1) was evaluated for mRNA and protein levels. LNCaP is androgen dependent, whereas PC3 and CWR22Rν1 are androgen independent. The normal immortalized cell line RWPE-1 was used to evaluate ASS expression in noncancerous prostate cells. All cell lines expressed ASS mRNA determined by reverse transcription-PCR (RT-PCR) except CWR22Rν1 (Fig. 1*A*). Quantitative real-time PCR of ASS mRNA in the prostate cancer cell lines revealed that, relative to CWR22Rν1, LNCaP and PC3 expressed ASS transcript 6.7 and 1.4 times greater, respectively. Western blot analysis showed CWR22Rν1 did not express ASS protein; in contrast, PC3 expressed moderate levels, whereas LNCaP and RWPE-1 expressed high levels of ASS (Fig. 1*B*). Disparity between ASS mRNA and protein levels is potentially attributed to nonproductive, alternatively spliced transcripts or pseudogenes.[7] The relationship between androgen status and ASS expression was further examined by treating LNCaP cells with 10 nmol/L DHT (Fig. 1*C*), revealing androgens do not regulate ASS expression.

To evaluate the effect of ADI-PEG20 on prostate carcinoma, the previously described cell lines were treated with ADI-PEG20 over a broad dose range and assayed for cytotoxicity with MTT. CWR22Rν1 was the most sensitive to ADI-PEG20 with an IC_{50} of 0.3 μg/mL. PC3 was moderately sensitive to ADI-PEG20, whereas LNCaP and RWPE-1 were not responsive to ADI-PEG20 (Fig. 1*D*). Taken together, these data confirm that ASS protein levels inversely correlate with sensitivity to ADI-PEG20. CWR22Rν1 was subsequently chosen as the model cell line for future experiments.

ADI-PEG20 induces caspase-independent apoptosis in CWR22Rv1 *in vitro*. To study whether the reduced viability of CWR22Rν1 upon ADI-PEG20 treatment is due to cell growth arrest, apoptosis, or both, we subjected treated and untreated cells to FACS analysis. The sub-G_1 DNA content was used as an indicator of apoptosis induced by ADI-PEG20. CWR22Rν1 cells were treated with 0.3 μg/mL ADI-PEG20 for 4, 24, 48, 72, and 96 hours. Apoptosis was not induced until 4 days posttreatment, when ~30% of cells had undergone apoptosis (Fig. 2*A*). Although DNA fragmentation is considered the defining end point in apoptosis, caspase cleavage is an early marker for classic apoptosis. Interestingly, cleavage of caspase-3 into its activated 17 kDa fragment was undetected after ADI-PEG20 (Fig. 2*B*).

Caspase-independent cell death was further investigated with z-VAD-fmk, a pan-caspase inhibitor. Caspase inhibition was confirmed with caspase-3 ELISA (Fig. 2*C*). z-VAD-fmk led to a 50%

[7] Pei-Jer Chen, personal communication.

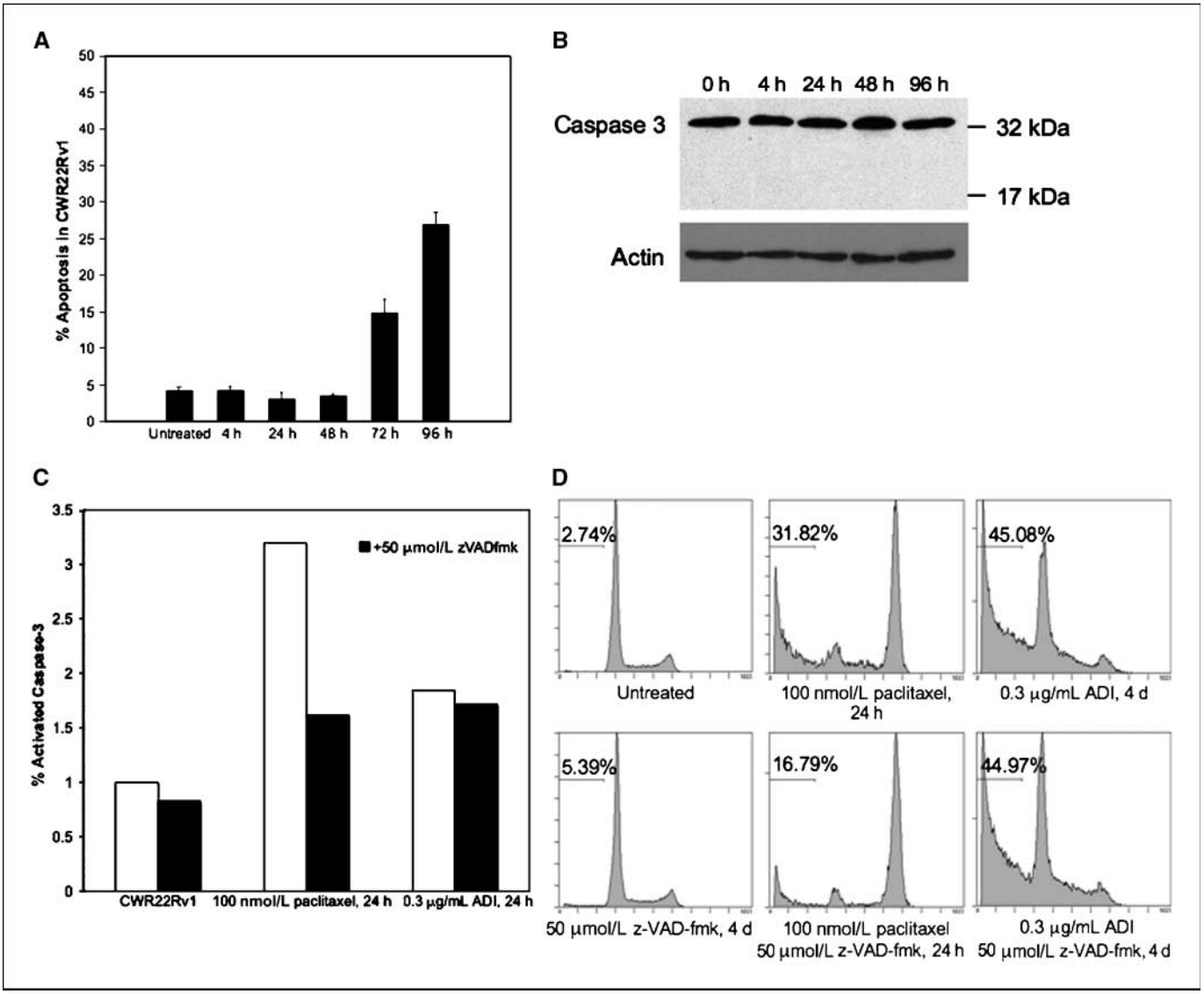

Figure 2. ADI-PEG20 induces caspase-independent apoptosis in CWR22R*v*1. *A,* 0.3 μg/mL ADI-PEG20 time course of CWR22R*v*1 before FACS analysis for sub-G_1 DNA content. *Columns,* mean; *bars,* SE. *B,* immunoblot for 0.3 μg/mL ADI-PEG20 time course of CWR22R*v*1. α-Caspase-3 detects the 32 kDa proform and the activated 17 kDa cleavage product. *C,* CWR22R*v*1 cells were treated with vehicle (untreated), 100 nmol/L paclitaxel, or 0.3 μg/mL ADI-PEG20 for 24 h and compared with 2 h pretreatment with 50 μmol/L z-VAD-fmk before caspase-3 ELISA. Values were normalized to vehicle. *D,* CWR22R*v*1 cells were treated with 50 μmol/L z-VAD-fmk, 0.3 μg/mL ADI-PEG20, ADI-PEG20+z-VAD-fmk for 96 h, and 100 nmol/L paclitaxel, paclitaxel+z-VAD-fmk for 24 h before FACS analysis for sub-G_1 DNA content.

reduction of activated caspase-3 levels in cells treated with paclitaxel, a standard chemotherapy for advanced and metastatic prostate cancer. However, ADI-PEG20 did not significantly alter active caspase-3 levels. Although z-VAD-fmk attenuated apoptosis in cells treated with paclitaxel by ~50%, it did not affect the fraction of apoptotic cells after ADI-PEG20 (Fig. 2*D*). These data suggest that cell death mediated by ADI-PEG20 is independent of caspase-mediated pathways.

ADI-PEG20 decreases global tumor metabolic activity. The immediate effect of ADI-PEG20 *in vivo* was examined using PET. Global tumor metabolism of glucose consumption was monitored by ^{18}F-fluorodeoxyglucose (^{18}F-FDG) in CWR22R*v*1 mouse xenografts. MicroPET scans were performed before and after ADI-PEG20 treatment of 4 or 24 hours. ^{18}F-FDG uptake in CWR22R*v*1 tumors (*arrows*) did not change after 4 hours of treatment. In contrast, ^{18}F-FDG uptake was decreased after 24 hours of ADI-PEG20. Tumor SUV decreased 30% after treatment (0.00086 versus 0.0006), indicating reduced metabolic activity (Fig. 3*A*).

ADI-PEG20 retards CWR22Rv1 tumor growth *in vivo* and synergizes with taxane. To determine the long term effects of ADI-PEG20 *in vivo*, nude athymic mice with s.c. CWR22R*v*1 xenografts were injected i.p. with control PBS or 5 IU ADI-PEG20 weekly. Tumors from ADI-PEG20 mice were significantly smaller than tumors from control mice (157.6 mm^3 versus 1,108.99 mm^3) at 13 days after initiation of treatment when control mice were euthanized. The effects of ADI-PEG20 were compared with the current standard of care for hormone refractory prostate cancer patients, docetaxel alone (27), and docetaxel in combination. Docetaxel mice (10 mg/kg) had tumors that were smaller but not statistically significant from control mice. However, the

combination of ADI-PEG20 and docetaxel had a synergistic effect on tumor growth inhibition. Tumors from ADI-PEG20 mice reached an average of 910 mm^3 at the end of the study, whereas tumors from ADI-PEG20/docetaxel–treated mice were ~75% smaller (Fig. 3*B*).

ADI-PEG20 induces autophagy in prostate cancer cells. Arginine degradation by ADI-PEG20 causes metabolic stress to auxotrophic cells. Nutrient starvation such as complete amino acid deprivation is a known inducer of autophagy (28). To determine whether single amino acid deprivation is sufficient to trigger autophagy, CWR22R*v*1 cells stably expressing eGFP-LC3 were examined under fluorescence microscopy. Under normal conditions, LC3-I is uniformly distributed throughout the nucleus and cytoplasm. During autophagy, LC3-I is processed into LC-II and translocates into autophagosome membranes, appearing as bright punctae (29). LC3-II localization was seen in fixed CWR22R*v*1 cells after 4 and 24 hours of 0.3 μg/mL ADI-PEG20 treatment. Rapamycin, an inhibitor of mTOR, was used as a positive control (Fig. 4*A, top*). Live cell imaging of CWR22R*v*1 cells revealed rapid and intense autophagosome formation after only 90 minutes of ADI-PEG20 (Fig. 4*A, bottom*). Rapamycin or ADI-PEG20 significantly increased the number of cells undergoing autophagy to 15%

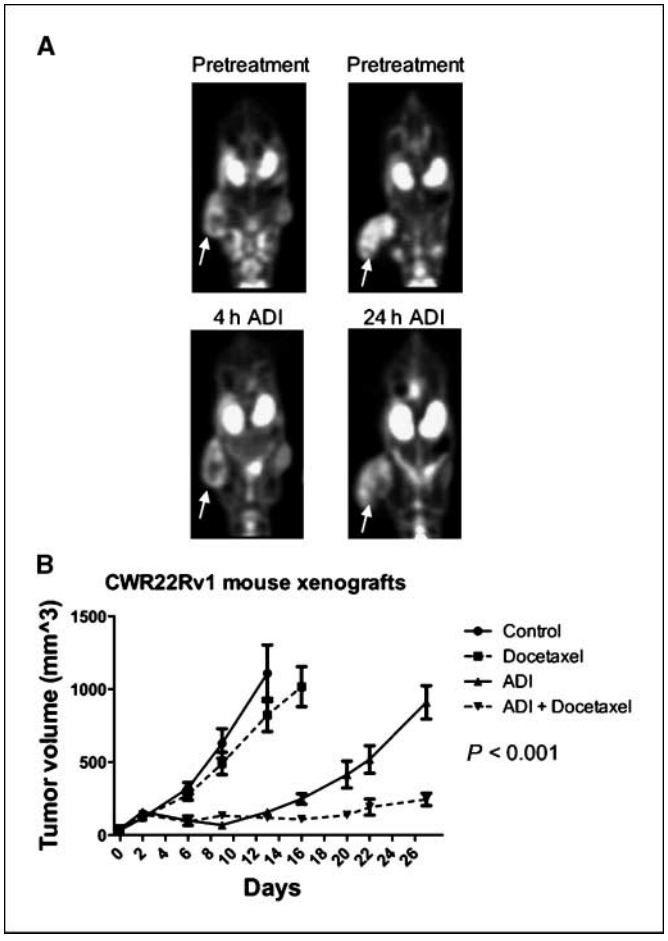

Figure 3. ADI-PEG20 is an effective agent *in vivo. A,* mice with CWR22R*v*1 xenografts were imaged by PET using ^{18}F-FDG before and after treatment with 5 IU ADI-PEG20 for 4 or 24 h. *B,* mice with CWR22R*v*1 xenografts were treated with PBS vehicle, 10 mg/kg docetaxel, 5 IU ADI-PEG20, or 5 IU ADI-PEG20+10 mg/kg docetaxel weekly. Tumor volumes are reported as mean ± SE.

(Fig. 4*A*). The LC3-II fragment appeared as early as 30 minutes of ADI-PEG20 and persisted after 24 hours of arginine deprivation. Increase in total autophagic flux was confirmed with chloroquine (30), an autophagy inhibitor that disrupts lysosomal function (Fig. 4*B*) and prevents completion of autophagy, resulting in an accumulation of LC3-II. In addition, potential off-target effects of chloroquine did not lead to caspase-3 cleavage.

Molecular pathways accompanying the induction of autophagy were also investigated. A major nutrient-sensing pathway involves AMPK/TSC/mTOR/S6K. During nutrient starvation, ATP level decreases and AMP level increases, resulting in activation and phosphorylation of AMPK. ADI-PEG20 immediately increased phospho-AMPK levels (Fig. 4*C*). This should lead to inactivation and decreased phosphorylation of mTOR kinase through the inhibition of TSC complex by AMPK-induced phosphorylation. Decreased phosphorylation of mTOR was evident soon after ADI-PEG20 treatment (Fig. 4*C*). A downstream mTOR effector, S6K, was inactivated at a later stage (>24 hours) as shown by its own decreased phosphorylation and the decreased phosphorylation of its substrate S6. Transient increase of S6K activity was observed at early ADI-PEG20 time points. The exact mechanism of this phenomenon is unclear but is likely due to feedback of this kinase as reported by others (31). AMPK activation and mTOR down-modulation are compatible with their roles of major autophagy regulators. We also surveyed other kinase pathways relevant to autophagy. ERK1/2 phosphorylation was evident within 30 minutes of ADI-PEG20 treatment, which increased in a time-dependent manner (Fig. 4*C*). ERK1/2 activation has been shown previously to contribute to autophagy induced prosurvival function (32).

Autophagy delays and protects against ADI-PEG20–induced cell death. The paradoxical relationship between autophagy and apoptosis necessitates determination of the causal nature between these two fundamental biological processes after arginine deprivation. Temporally, autophagy precedes apoptosis; thus, inhibition of autophagy may modulate the onset of apoptosis.

Chemical inhibition of autophagy with chloroquine accelerated and enhanced ADI-PEG20–induced cell death in CWR22R*v*1 (Fig. 5*A*). By 48 hours, 27% of ADI-PEG20 + chloroquine cells were apoptotic compared with 11% and 6% of cells undergoing apoptosis by chloroquine alone and ADI-PEG20 alone, respectively. Chloroquine further increased ADI-PEG20–induced cell death to 60% after 72 hours. By 96 hours, the effect of chloroquine was abrogated, possibly due to its metabolism. Similarly, siRNA knockdown of Beclin1, essential for autophagosome nucleation (21), also increased the rate of cell death after ADI-PEG20 treatment (Fig. 5*B*). Almost 60% of cells had undergone apoptosis if Beclin1 was knocked down before 48 hours of ADI-PEG20, whereas ADI-PEG20 alone only led to apoptosis in 30% of cells. In contrast, ADI-PEG20, chloroquine, and the combination of ADI-PEG20 and chloroquine had no effect on apoptosis at all time points in the ASS expressing LNCaP cells (Fig. 5*C*). To complete the characterization of the relationship of ASS expression and sensitivity to ADI-PEG20, we examined cellular response in PC3, a cell line with low ASS levels. Higher doses of ADI-PEG20 (5 μg/mL) were required to arrest cell growth completely compared with CWR22R*v*1, although lower doses (0.3 μg/mL) induced autophagy (Fig. 5*D*). Inhibiting autophagy with 3-MA greatly reduced cell viability following treatment with low dose ADI-PEG20 (Fig. 5*D*). Therefore, ASS protein level correlates with cellular response to ADI-PEG20, including the early induction of autophagy before the late onset of apoptosis.

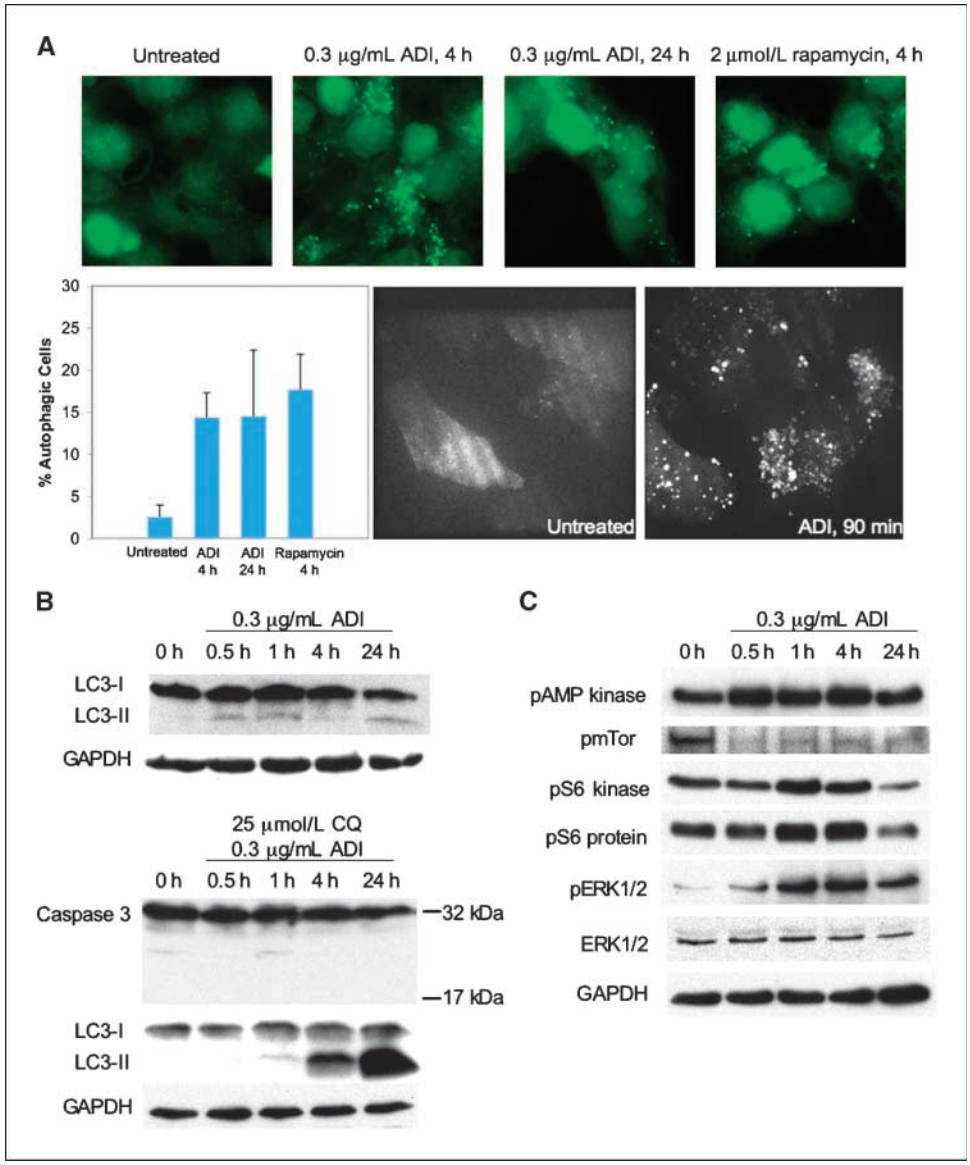

Figure 4. ADI-PEG20 induces autophagy in CWR22R*v*1. *A,* CWR22R*v*1 cells overexpressing eGFP-LC3 were treated with 0.3 μg/mL ADI-PEG20 for 1.5, 4, and 24 h, or 2 μmol/L rapamycin for 4 h. Punctae represent autophagosome formation. Autophagic cells were quantified from random image fields totaling 200 cells and reported as mean ± SE. *B,* immunoblot for 0.3 μg/mL ADI-PEG20 time course of CWR22R*v*1. α-LC3 detects LC3-I and LC3-II. Autophagic flux was confirmed by coadministering 25 μmol/L chloroquine with 0.3 μg/mL ADI-PEG20. α-Caspase-3 detects the 32 kDa proform and the activated 17 kDa cleavage product. *C,* immunoblot for 0.3 μg/mL ADI-PEG20 time course of CWR22R*v*1 using α-phopsho-AMP kinase, α-phospho-mTor, α-phospho-S6 kinase, α-phospho-S6 protein, α-phospho-ERK1/2, and α-ERK1/2. Loading control for phospho-mTor was verified using α-tubulin (data not shown).

ASS expression in prostate cancer tissue. The above results suggest arginine deprivation by ADI-PEG20 may offer a new treatment strategy for prostate cancers in which ASS expression is low. A key question that follows is whether the absence of ASS expression is generalizable among diverse human prostate cancer specimens. We therefore examined ASS expression by immunohistochemistry in our prostate tissue microarray. Of the 88 human prostate tumors, none showed any detectable ASS staining. Strong cytoplasmic ASS staining was observed, indicated by closed arrows, in the luminal cells of benign prostate glands (Fig. 6*A*) and normal prostate tissue (Fig. 6*B, left*). However, no ASS reactivity was detected in prostate cancer glands (Fig. 6*A, open arrows*) or tissue (Fig. 6*B, right*). Among 59 samples of normal prostate tissue, 27% expressed ASS to some degree. Of the 16 samples showing ASS expression, 2 were found to have ASS in >75% of the cells, whereas the remaining 14 showed expression in <25% of the cells. In addition, ASS mRNA expression was evaluated in six primary prostate tumor tissues and two primary benign prostatic hyperplasia tissues. ASS mRNA was almost absent in specimen 108 and reduced in all other samples (Fig. 6*C*). The differential expression of ASS is in contrast to hepatocytes, which heavily depend on ASS function for the urea cycle, and uniformly stained for cytoplasmic ASS protein (Fig. 6*D*).

Discussion

In this report, we showed ADI-PEG20 can effectively induce cell death in prostate cancer cells with low or absent ASS expression. It also sensitizes cells to treatment with docetaxel, an accepted chemotherapy in prostate cancer, or chloroquine, an inhibitor of autophagy. These results are likely to be generally applicable to other prostate cancer cells because virtually all prostate cancer specimens examined in this report as well as that by Clark and colleagues (12) expressed undetectable levels of ASS. By depletion of arginine, ADI-PEG20 causes metabolic stress on auxotrophic cells, complimenting conventional therapies largely based on genotoxic stress. Although arginine deprivation therapy based on bovine arginase has seen limited applications clinically, ADI-PEG20

has 1,000-fold greater affinity for arginine (33) with fewer side effects. Our work described here thus offers a new treatment option for prostate cancer. In addition, we uncover novel cellular responses of arginine depletion, including autophagy and caspase-independent cell death.

The delayed onset of apoptosis suggests the possibility of compensation mechanisms after arginine depletion. Here, we present evidence for the first time that single amino acid starvation through arginine degradation by ADI-PEG20 is sufficient to trigger autophagy in prostate cancer cells. LC3 translocation and cleavage occur within hours of ADI-PEG20 treatment, indicating that autophagy is an early response. AMPK senses cellular AMP/ATP ratio, and in its phosphorylated form, signals the lack of nutrients in the environment to the mTOR complex via TSC2 (34). Inhibition of mTOR leads to suppression of S6K activity. Consistent with our findings, Feun and colleagues (35) have reported the effects of ADI-PEG20 on mTOR signaling, which include dephosphorylation of mTOR downstream effectors S6K and 4E-BP and increased phosphorylation of AMPK in ASS-negative melanoma cell lines. This chain of events has been shown to promote autophagy (36). There are various signaling cascades that regulate mTOR/S6K including the PI3K (class I)/Akt pathway; inhibition of which has been shown to induce autophagy in malignant gliomas (32, 37). Although we did not specifically examine the activation of the PI3K (class I)/Akt pathway, ADI-PEG20 inhibited mTOR events associated with a rapid activation of AMPK, suggesting this mechanism in arginine deprivation-induced autophagy. Furthermore, we observed ADI-PEG20–induced ERK1/2 activation, which has been shown to regulate autophagy under a variety of stimuli (32, 38).

What is the biological function of ADI-PEG20 induced autophagy? Autophagy can be prosurvival or prodeath, depending on cellular context and duration of treatment. To study whether ADI-PEG20 induced autophagy contributes to or attenuates cell death, we chose to block ADI-PEG20 induced autophagy with the inhibitor chloroquine, which inhibits late stage autophagy by alkalinizing lysosomes and disrupting the autophagolysosome (39). Because chloroquine itself may have functions other than inactivating lysosomes (40), we also used siRNA targeting an essential component of autophagy, Beclin1, a component of the class III PI3 kinase complex that nucleates autophagosomes (29).

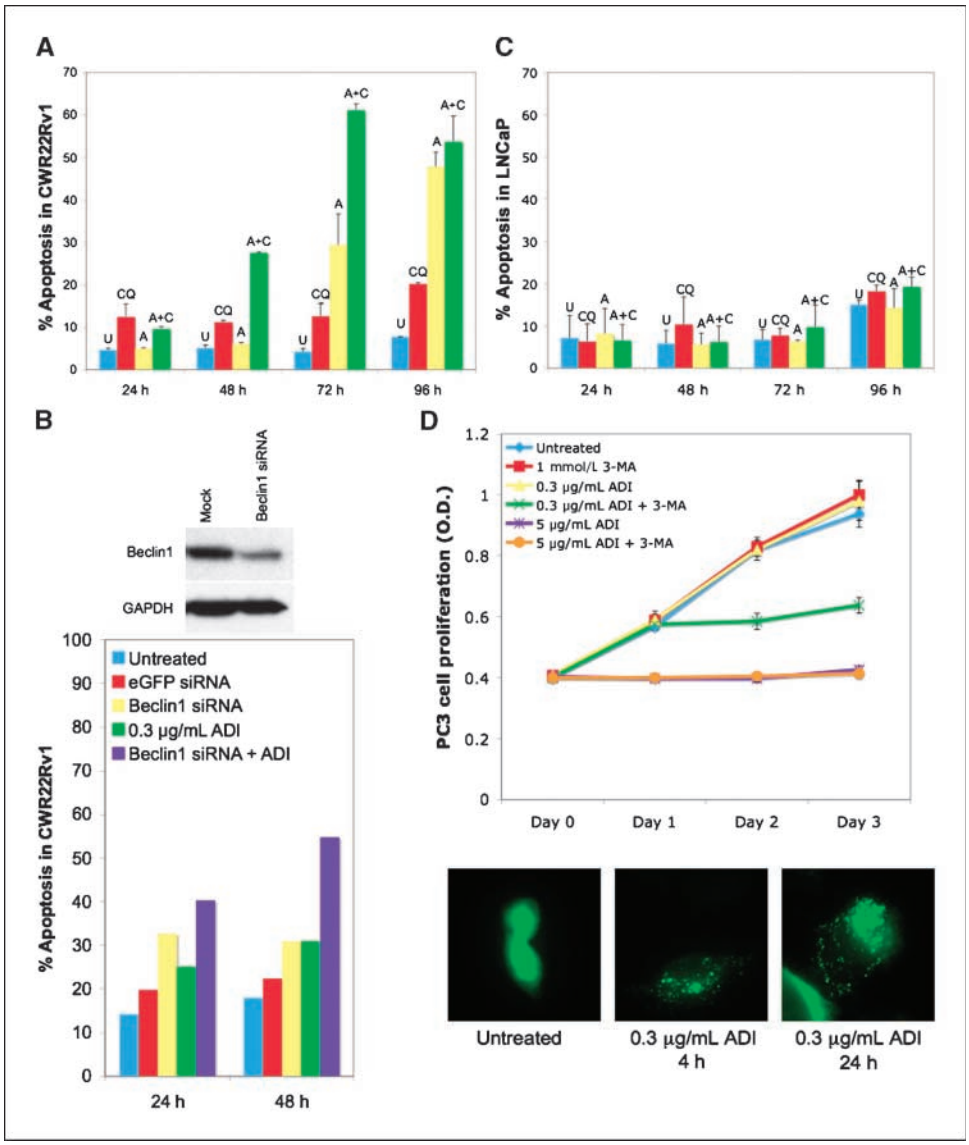

Figure 5. Inhibition of autophagy accelerates and enhances ADI-PEG20–induced cell death. *A,* time course of CWR22R*v*1 cells treated with vehicle (untreated), 25 μmol/L CQ, 0.1 μg/mL ADI-PEG20, or ADI-PEG20+CQ before FACS analysis for sub-G_1 content. *Columns,* mean; *bars,* SE. *B,* immunoblot for CWR22R*v*1 cells transfected with mock or 100 pmol Beclin1 siRNA to assess knockdown. CWR22R*v*1 cells were treated with vehicle (untreated), 0.3 μg/mL ADI-PEG20, 100 pmol eGFP siRNA, 100 pmol Beclin1 siRNA, or Beclin1 siRNA+ADI-PEG20 for 24 and 48 h before FACS analysis for sub-G_1 content. *C,* LNCaP cells were treated and analyzed as described in *A* with 0.3 μg/mL ADI-PEG20. *D,* growth of PC3 cells were treated with vehicle (untreated), 0.3 μg/mL ADI-PEG20, 1 mmol/L 3-MA, 0.3 μg/mL ADI-PEG20+1 mmol/L 3-MA, 5 μg/mL ADI-PEG20, or 5 μg/mL ADI-PEG20+1 mmol/L 3-MA by MTT assay. *Points,* mean; *bars,* SD. PC3 cells overexpressing eGFP-LC3 were treated with 0.3 μg/mL ADI-PEG20 for 4 or 24 h. Punctae represent autophagosome formation. *U,* untreated; *CQ,* chloroquine; *A,* ADI-PEG20.

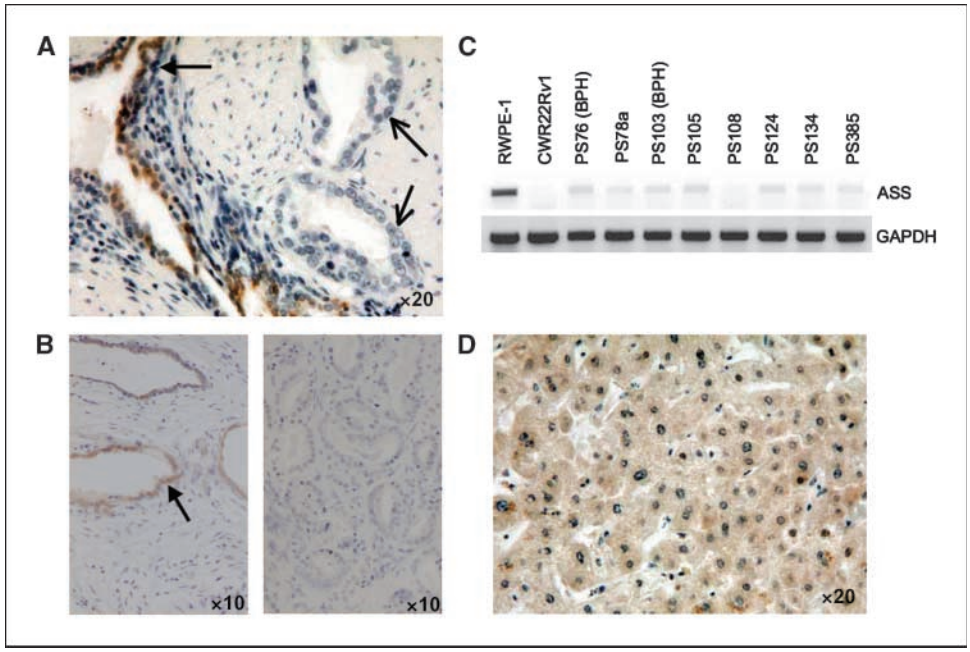

Figure 6. ASS expression in prostate tissue. *A,* prostate cancer tissue with ASS(+) benign glands (closed arrows) and ASS(−) cancerous glands (*open arrows*) by immunohistochemistry. *B, left,* normal prostate tissue. *Closed arrows,* luminal ASS staining. *Right*, prostate cancer tissue with no ASS reactivity. *C,* mRNA from primary prostate tissue was examined for ASS expression by RT-PCR. *D,* normal liver as a positive control for cytoplasmic ASS staining. *BPH,* benign prostatic hyperplasia.

Our data show inhibition of early stage autophagy by chloroquine or Beclin1 knockdown accelerates and enhances cell death after ADI-PEG20, strongly suggesting ADI-PEG20–induced autophagy triggers a protective response during early stages of treatment. At present, we cannot rule out that prolonged ADI-PEG20 treatment (>96 hours) may trigger autophagic cell death (programmed cell death type II), which is usually caspase-independent. In our study, we found chloroquine itself had little effect on the cell killing of CWR22R*v*1, unless ADI-PEG20 is present and autophagy is induced. In addition, coadministration of chloroquine with ADI-PEG20 did not activate caspase-3. This again suggests that the major effect of chloroquine is to block autophagy, enhancing the underlying mechanism of caspase-independent apoptosis. Consistent with this result, PC3 cells with reduced ASS levels also underwent autophagy after ADI-PEG20 treatment. The inhibition of autophagy with 3-MA significantly reduced cell proliferation in the presence of ADI-PEG20. Both chloroquine and ADI-PEG20 have no effect on LNCaP cells, which express ASS. Interestingly, ASS-positive hepatocellular carcinomas resistant to ADI-PEG20 responded to arginine deprivation by pegylated recombinant arginase (41), providing a potential alternative to ADI-PEG20–resistant tumors and cell lines such as LNCaP.

In cancer, an autophagy paradox has emerged in which survival and death are context specific, particularly due to complex interactions between autophagic and apoptotic pathways. Accordingly, cancer therapies have been reported to have opposing effects on cell death. Photodynamic therapy promotes autophagic cell death in apoptosis-deficient cancer cells (42), whereas sulforaphane-induced autophagy in PC3 and LNCaP is protective (43). Furthermore, manipulation of autophagy can sensitize tumor cells to subsequent treatments. Induction of autophagy by an mTOR inhibitor increased prostate cancer cell susceptibility to irradiation (44). Conversely, chloroquine is a highly promising autophagy inhibitor for clinical use. Although it is extensively used to treat malaria (20), its uses against cancer are only recently emerging. In a *myc*-induced lymphoma model, autophagic inhibition by chloroquine enhanced the ability of alkylating agents to suppress tumor growth (45). This underscores the importance of autophagy to fundamental cell processes and its ability to modulate the effect of chemotherapies across a wide variety of cancers.

The absence of ASS as a biomarker for ADI-PEG20 efficacy has previously been established in hepatoma and melanoma cell lines. Phase I/II clinical trials with ADI-PEG20 led to a 47% response rate in patients with unresectable hepatocellular carcinomas and a 25% response rate in metastatic melanoma patients (46, 47). In this study, we show ADI-PEG20 can be effective against prostate cancer. ASS expression can be determined by immunohistochemistry and potentially be used as a clinical indicator for ADI-PEG20 use. The absence of ASS protein in all examined prostate tumor samples makes ADI-PEG20 a promising therapeutic avenue to follow. The combination of ADI-PEG20, which induces caspase-independent apoptosis, and taxanes, which are caspase-dependent, is more effective than monotherapy. This concept of synergistic interaction between cancer therapies is an active area of research. In particular, combining therapies that target different mechanisms of cell death may increase efficacy beyond either agent alone. Furthermore, the increase of advanced imaging for tumor assessment and staging may allow clinical monitoring of tumor responsiveness to ADI-PEG20 by PET. Finally, arginine deprivation by ADI-PEG20 induces autophagy as a protective mechanism. Coadministration with an autophagic inhibitor such as chloroquine can potentially enhance cell death in prostate tumors. The intricate link between autophagy and apoptosis points to autophagy as an additional target for anticancer treatments. Thus, ADI-PEG20 is a novel prostate cancer therapy whose mechanism of action can be complemented by other chemotherapies to maximize cell death.

Disclosure of Potential Conflicts of Interest

R.J. Bold: commercial research grant, DesigneRx Pharmaceuticals. The other authors disclosed no potential conflicts of interest.

Acknowledgments

Received 8/14/2008; revised 10/15/2008; accepted 10/31/2008.

Grant support: NIH DK52659 and CA114575 (H.J. Kung), 5TL1RR024145-02 (R.H. Kim); DOD W81XWH-08-1-0167 (R.H. Kim), and a research agreement by DesigneRx Pharmaceuticals, Inc (R.J. Bold). H.J. Kung also acknowledges the support of the Auburn Community Cancer Endowment Fund.

The costs of publication of this article were defrayed in part by the payment of page charges. This article must therefore be hereby marked *advertisement* in accordance with 18 U.S.C. Section 1734 solely to indicate this fact.

We thank the support and reagents provided by Dr. Jenny Wei-Jen Kung, Dr. Liang Xia, Dr. Bor-Wen Wu, and Dr. John Bomalaski; Subbulakshmi Virudachalam for technical advice; Dr. Ai-Hong Ma for initially testing the avidity of ASS antibody; and Dr. Ralph DeVere White for providing total RNA from primary prostate tissue.

References

1. Miyazaki K, Takaku H, Umeda M, et al. Potent growth inhibition of human tumor cells in culture by arginine deiminase purified from a culture medium of a Mycoplasma-infected cell line. Cancer Res 1990;50:4522–7.

2. Takaku H, Matsumoto M, Misawa S, Miyazaki K. Antitumor activity of arginine deiminase from Mycoplasma argini and its growth-inhibitory mechanism. Jpn J Cancer Res 1995;86:840–6.

3. Takaku H, Takase M, Abe S, Hayashi H, Miyazaki K. *In vivo* anti-tumor activity of arginine deiminase purified from Mycoplasma arginini. Int J Cancer 1992;51:244–9.

4. Ensor CM, Holtsberg FW, Bomalaski JS, Clark MA. Pegylated arginine deiminase (ADI-SS PEG20,000 mw) inhibits human melanomas and hepatocellular carcinomas *in vitro* and *in vivo*. Cancer Res 2002;62:5443–50.

5. Holtsberg FW, Ensor CM, Steiner MR, Bomalaski JS, Clark MA. Poly(ethylene glycol) (PEG) conjugated arginine deiminase: effects of PEG formulations on its pharmacological properties. J Control Release 2002;80:259–71.

6. Szlosarek PW, Klabatsa A, Pallaska A, et al. *In vivo* loss of expression of argininosuccinate synthetase in malignant pleural mesothelioma is a biomarker for susceptibility to arginine depletion. Clin Cancer Res 2006;12:7126–31.

7. Yoon CY, Shim YJ, Kim EH, et al. Renal cell carcinoma does not express argininosuccinate synthetase and is highly sensitive to arginine deprivation via arginine deiminase. Int J Cancer 2007;120:897–905.

8. Bowles TL, Kim R, Galante J, et al. Pancreatic cancer cell lines deficient in argininosuccinate synthetase are sensitive to arginine deprivation by arginine deiminase. Int J Cancer 2008;123:1950–5.

9. Husson A, Brasse-Lagnel C, Fairand A, Renouf S, Lavoinne A. Argininosuccinate synthetase from the urea cycle to the citrulline-NO cycle. Eur J Biochem 2003;270:1887–99.

10. Lind DS. Arginine and cancer. J Nutr 2004;134:2837–41S; discussion 53S.

11. Shen LJ, Beloussow K, Shen WC. Modulation of arginine metabolic pathways as the potential anti-tumor mechanism of recombinant arginine deiminase. Cancer Lett 2006;231:30–5.

12. Dillon BJ, Prieto VG, Curley SA, et al. Incidence and distribution of argininosuccinate synthetase deficiency in human cancers: a method for identifying cancers sensitive to arginine deprivation. Cancer 2004;100:826–33.

13. Gong H, Zolzer F, von Recklinghausen G, et al. Arginine deiminase inhibits cell proliferation by arresting cell cycle and inducing apoptosis. Biochem Biophys Res Commun 1999;261:10–4.

14. Beloussow K, Wang L, Wu J, Ann D, Shen WC. Recombinant arginine deiminase as a potential anti-angiogenic agent. Cancer Lett 2002;183:155–62.

15. Gong H, Pottgen C, Stuben G, Havers W, Stuschke M, Schweigerer L. Arginine deiminase and other antiangiogenic agents inhibit unfavorable neuroblastoma growth: potentiation by irradiation. Int J Cancer 2003;106:723–8.

16. Levine B, Klionsky DJ. Development by self-digestion: molecular mechanisms and biological functions of autophagy. Dev Cell 2004;6:463–77.

17. Mizushima N, Levine B, Cuervo AM, Klionsky DJ. Autophagy fights disease through cellular self-digestion. Nature 2008;451:1069–75.

18. Kabeya Y, Mizushima N, Ueno T, et al. LC3, a mammalian homologue of yeast Apg8p, is localized in autophagosome membranes after processing. EMBO J 2000;19:5720–8.

19. Mathew R, Karantza-Wadsworth V, White E. Role of autophagy in cancer. Nat Rev Cancer 2007;7:961–7.

20. Amaravadi RK, Thompson CB. The roles of therapy-induced autophagy and necrosis in cancer treatment. Clin Cancer Res 2007;13:7271–9.

21. Pattingre S, Espert L, Biard-Piechaczyk M, Codogno P. Regulation of macroautophagy by mTOR and Beclin 1 complexes. Biochimie 2008;90:313–23.

22. Maiuri MC, Criollo A, Tasdemir E, et al. BH3-only proteins and BH3 mimetics induce autophagy by competitively disrupting the interaction between Beclin 1 and Bcl-2/Bcl-X(L). Autophagy 2007;3:374–6.

23. Crighton D, Wilkinson S, O'Prey J, et al. DRAM, a p53-induced modulator of autophagy, is critical for apoptosis. Cell 2006;126:121–34.

24. Gozuacik D, Kimchi A. DAPk protein family and cancer. Autophagy 2006;2:74–9.

25. Desai SJ, Ma AH, Tepper CG, Chen HW, Kung HJ. Inappropriate activation of the androgen receptor by nonsteroids: involvement of the Src kinase pathway and its therapeutic implications. Cancer Res 2006;66:10449–59.

26. Parsons CM, Sutcliffe JL, Bold RJ. Preoperative evaluation of pancreatic adenocarcinoma. J Hepatobiliary Pancreat Surg 2008;15:429–35.

27. Van Poppel H. Recent docetaxel studies establish a new standard of care in hormone refractory prostate cancer. Can J Urol 2005;12 Suppl 1:81–5.

28. Mortimore GE, Schworer CM. Induction of autophagy by amino-acid deprivation in perfused rat liver. Nature 1977;270:174–6.

29. Liang C, Feng P, Ku B, et al. Autophagic and tumour suppressor activity of a novel Beclin1-binding protein UVRAG. Nat Cell Biol 2006;8:688–99.

30. Mizushima N, Yoshimori T. How to interpret LC3 immunoblotting. Autophagy 2007;3:542–5.

31. Codogno P, Meijer AJ. Autophagy and signaling: their role in cell survival and cell death. Cell Death Differ 2005;12 Suppl 2:1509–18.

32. Shinojima N, Yokoyama T, Kondo Y, Kondo S. Roles of the Akt/mTOR/p70S6K and ERK1/2 signaling pathways in curcumin-induced autophagy. Autophagy 2007;3:635–7.

33. Dillon BJ, Holtsberg FW, Ensor CM, Bomalaski JS, Clark MA. Biochemical characterization of the arginine degrading enzymes arginase and arginine deiminase and their effect on nitric oxide production. Med Sci Monit 2002;8:BR248–53.

34. Hardie DG. The AMP-activated protein kinase pathway-new players upstream and downstream. J Cell Sci 2004;117:5479–87.

35. Feun L, You M, Wu CJ, et al. Arginine deprivation as a targeted therapy for cancer. Curr Pharm Des 2008;14:1049–57.

36. Xu ZX, Liang J, Haridas V, et al. A plant triterpenoid, avicin D, induces autophagy by activation of AMP-activated protein kinase. Cell Death Differ 2007;14:1948–57.

37. Aoki H, Takada Y, Kondo S, Sawaya R, Aggarwal BB, Kondo Y. Evidence that curcumin suppresses the growth of malignant gliomas *in vitro* and *in vivo* through induction of autophagy: role of Akt and extracellular signal-regulated kinase signaling pathways. Mol Pharmacol 2007;72:29–39.

38. Pattingre S, Bauvy C, Codogno P. Amino acids interfere with the ERK1/2-dependent control of macroautophagy by controlling the activation of Raf-1 in human colon cancer HT-29 cells. J Biol Chem 2003;278:16667–74.

39. Maiuri MC, Zalckvar E, Kimchi A, Kroemer G. Self-eating and self-killing: crosstalk between autophagy and apoptosis. Nat Rev 2007;8:741–52.

40. Maclean KH, Dorsey FC, Cleveland JL, Kastan MB. Targeting lysosomal degradation induces p53-dependent cell death and prevents cancer in mouse models of lymphomagenesis. J Clin Invest 2008;118:79–88.

41. Cheng PN, Lam TL, Lam WM, et al. Pegylated recombinant human arginase (rhArg-peg5,000mw) inhibits the *in vitro* and *in vivo* proliferation of human hepatocellular carcinoma through arginine depletion. Cancer Res 2007;67:309–17.

42. Xue LY, Chiu SM, Azizuddin K, Joseph S, Oleinick NL. Protection by Bcl-2 against apoptotic but not autophagic cell death after photodynamic therapy. Autophagy 2008;4:125–7.

43. Herman-Antosiewicz A, Johnson DE, Singh SV. Sulforaphane causes autophagy to inhibit release of cytochrome C and apoptosis in human prostate cancer cells. Cancer Res 2006;66:5828–35.

44. Cao C, Subhawong T, Albert JM, et al. Inhibition of mammalian target of rapamycin or apoptotic pathway induces autophagy and radiosensitizes PTEN null prostate cancer cells. Cancer Res 2006;66:10040–7.

45. Amaravadi RK, Yu D, Lum JJ, et al. Autophagy inhibition enhances therapy-induced apoptosis in a Myc-induced model of lymphoma. J Clin Invest 2007;117:326–36.

46. Izzo F, Marra P, Beneduce G, et al. Pegylated arginine deiminase treatment of patients with unresectable hepatocellular carcinoma: results from phase I/II studies. J Clin Oncol 2004;22:1815–22.

47. Ascierto PA, Scala S, Castello G, et al. Pegylated arginine deiminase treatment of patients with metastatic melanoma: results from phase I and II studies. J Clin Oncol 2005;23:7660–8.

[Autophagy 5:4, 1-2; 16 May 2009]; ©2009 Landes Bioscience

Autophagic Punctum

ADI, autophagy and apoptosis

Metabolic stress as a therapeutic option for prostate cancer

Randie H. Kim,[1] Richard J. Bold[2] and Hsing-Jien Kung[1,*]

[1]Department of Biological Chemistry; [2]Department of Surgery (Division of Surgical Oncology); University of California-Davis; Sacramento, CA USA

Key words: autophagy, arginine deiminase, arginine deprivation, caspase-independent apoptosis, prostate cancer

Prostate cancer, the leading incidence of cancer in American males, is a disease in which treatment of nonlocalized tumors remains largely unsuccessful. These cancers lose expression of an arginine synthesis enzyme, argininosuccinate synthetase (ASS), and are susceptible to arginine deprivation by arginine deiminase (ADI). We show CWR22R*v*1 prostate cancer cells are susceptible to ADI in a caspase-independent manner in vitro and in a xenograft model in vivo. We demonstrate that single amino acid deprivation by ADI is able to trigger autophagy. Inhibition of autophagy by chloroquine and siRNA enhances and accelerates ADI-induced cell death, suggesting that autophagy is a protective response to ADI, at least in the early phases. In addition, the co-administration of docetaxel, a caspase-dependent chemotherapy, with ADI inhibits tumor growth in vivo. Thus, targeting multiple cell death pathways, either through autophagy modulation or non-canonical apoptosis, may find expanded use as adjuvant chemotherapies, providing additional avenues for cancer treatment.

Recently, there is renewed interest in agents that cause metabolic stress as an alternative or adjunctive therapy for cancer to overcome resistance to conventional genotoxic agents. Amino acid deprivation as an anticancer therapy has long been recognized. A well-known example is asparagine-deprivation by asparaginase for acute lymphoblastic leukemias. Similarly, arginase-based treatment for lymphosarcoma and hepatoma has been reported in experimental models. Arginase, however, has received little attention clinically, due to sub-optimal properties of the purified enzyme from bovine tissues. Arginine is a semi-essential amino acid that is manufactured by the enzyme ASS (argininosuccinate synthetase) (Fig. 1). For reasons not well understood, in the development of certain cancers there is a selection against ASS expression, rendering the cancer cells auxotrophic for arginine. Consequently, arginine depletion by either arginase or arginine deiminase (ADI) will lead to selective tumor cell death.

ADI is an enzyme isolated from *Mycoplasma* that effectively metabolizes arginine into citrulline. At physiological pH, ADI is 300x more effective than arginase at depleting arginine. Antigenicity is decreased by conjugation to polyethylene glycol (PEG), which also increases enzyme half-life. Pegylated modification of recombinant ADI (DesigneRx, California) has dramatically improved its prospects as a therapeutic agent. PEG-ADI is efficacious against hepatocellular carcinomas and melanomas in vitro and in vivo. In particular, phase I/II clinical trials in these patients yield significant response rates with mild side effects. The efficacy of ADI on hepatocellular carcinomas and melanomas is correlated with ASS deficiency. Strikingly, in our analysis of 88 prostate cancer specimens, none expressed ASS. Figure 2 illustrates the lack of ASS expression in tumor cells compared to the high expression found in the surrounding normal prostate epithelium.

We first tested the ADI effect on various prostate cancer cell lines and found ADI sensitivity was inversely proportional to ASS protein levels. CWR22R*v*1, a castration-resistant prostate cancer cell line that does not express ASS, is highly sensitive to ADI-induced killing. We then extended these studies in vivo with CWR22R*v*1 xenografts in nude mice. Weekly injections of ADI resulted in the complete suppression of tumor growth, indicating the effectiveness of ADI as a treatment option for prostate cancer.

The ADI-induced cell killing of CWR22R*v*1 is atypical in at least two aspects: first, it is caspase-independent, and second, it follows a delayed kinetics with very little cell killing in the first 48 hours. Although nutritional starvation is known to induce autophagy, the effect of single amino acid removal such as arginine has not been as well documented. We therefore set forth to test whether ADI induces autophagy in CWR22R*v*1. By GFP-LC3 (a marker for autophagosomes) under fluorescence microscopy and the generation of LC3-II by western, the induction of autophagy was detected as early as 30 minutes after ADI treatment. Time-lapse images of CWR22R*v*1 cells overexpressing GFP-LC3 and RFP-LAMP-1 (a marker for lysosomes) using live cell fluorescence microscopy revealed the rapid appearance of large, bright puncta as well as dynamic colocalization with lysosomes over time (Fig. 3). Advanced quantitative parameters

*Correspondence to: Hsing-Jien Kung; UC Davis Cancer Center; University of California—Davis Medical Center; Research III; Room 2400B; 4645 2nd Avenue; Sacramento, CA 95817 USA; Tel.: 916.734.1538; Fax: 916.734.2589; Email: hkung@ucdavis.edu

Submitted: 02/04/09; Revised: 02/19/09; Accepted: 02/20/09

Previously published online as an *Autophagy* E-publication: http://www.landesbioscience.com/journals/autophagy/article/8252

Punctum to: Kim RH, Coates JM, Bowles TL, McNerney GP, Sutcliffe J, Jung JU, Gandour-Edwards R, Chuang FYS, Bold RJ, Kung HJ. Arginine deiminase as a novel therapy for prostate cancer induces autophagy and caspase-independent apoptosis. Cancer Res 2009; 69:700-708; PMID: 19147587; DOI: 10.1158/0008-5472.CAN-08-3157.

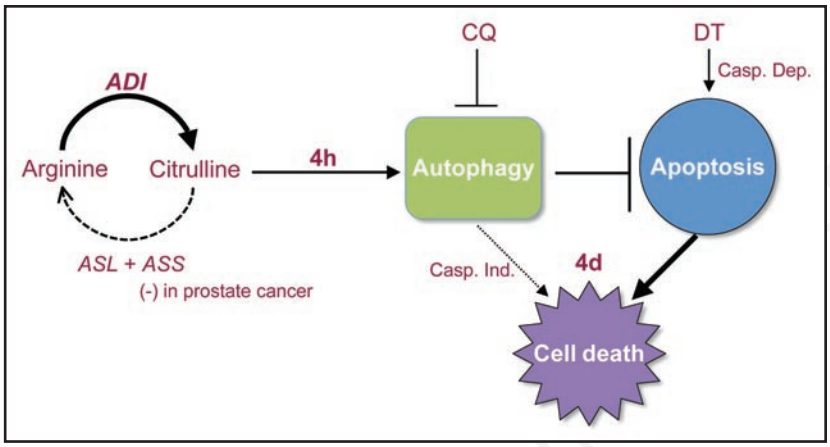

Figure 1. Proposed model of ADI-induced cell death. Arginine is synthesized in a two-step process catalyzed by the rate-limiting enzyme argininosuccinate synthetase (ASS) and argininosuccinate lyase (ASL). Arginine deiminase (ADI) hydrolyzes arginine back into its citrulline precursor (solid arrow). In prostate tumors that lack ASS, citrulline cannot re-enter the arginine synthesis pathway (dashed arrow), resulting in the depletion of intracellular arginine and the accumulation of citrulline upon ADI treatment. ADI treatment leads to a rapid induction of autophagy (4 hours) as a protective response to delay apoptosis at 4 days. Prolonged autophagy, however, may also contribute to caspase-independent cell death (dotted arrow). Cell death can be enhanced using chloroquine (CQ), an autophagic inhibitor, or docetaxel (DT), a caspase-dependent apoptotic inducer.

extracted from 4D images of autophagosomes may reflect potentially different mechanistic pathways of autophagy. Detailed analysis of ADI-treated CWR22R*v*1 cells revealed AMPK and ERK activation, and AKT, mTOR and S6K attenuation. Cells can, therefore, mount a strong autophagic response even to single amino acid depletion.

The relationship between autophagy and apoptosis after ADI treatment was investigated. siRNA knockdown of *beclin 1* enhanced ADI-induced apoptosis at both 24 and 48 hours, suggesting that autophagy, at least in the early phase, serves to protect cells from apoptosis. Additionally, we used chloroquine, a clinically approved antimalarial drug known to inactivate lysosomal functions, to interfere with the autophagic process. Chloroquine also accelerated apoptotic death induced by ADI. Our results suggest a protective role of autophagy in the initial phase of ADI-induced apoptosis, and the potential of using ADI/chloroquine combination therapy to enhance the killing of tumor cells.

The chemotherapeutic agent docetaxel represents one of the few options for treating hormone-resistant prostate cancer. Since docetaxel induces cell killing via caspases, leading to induction of traditional apoptosis, we determined in vivo whether ADI may complement docetaxel in cell killing via a caspase-independent mechanism. Whereas each therapy slowed growth of CWR22R*v*1 xenografts, the ADI/docetaxel combination showed a dramatic reduction of tumor growth compared to the groups receiving individual therapies. Although we have yet to examine ADI/chloroquine combination therapy in vivo, chloroquine has emerged as an anticancer autophagy modulator in other in vivo models. Combination therapy is currently very attractive for several reasons. In addition to increased efficacy, combination therapy may circumvent or delay the emergence of resistant tumors or improve patient quality of life by reducing side effects associated with high concentrations of chemotherapy drugs.

In summary, we present a new therapy for prostate cancer, based on the interesting finding that most, if not all, prostate cancers are auxotrophic for arginine. At present, we do not understand why prostate cancer cells are selected against ASS expression, nor do we know the initial mechanism whereby ADI triggers autophagy and caspase-independent apoptosis. Increasing evidence suggests that autophagic death induced by metabolic stress utilizes pathways largely different from the caspase-dependent genotoxic agents. Targeting disparate mechanisms appears beneficial, implying that the interaction of autophagy and apoptosis has therapeutic rationale.

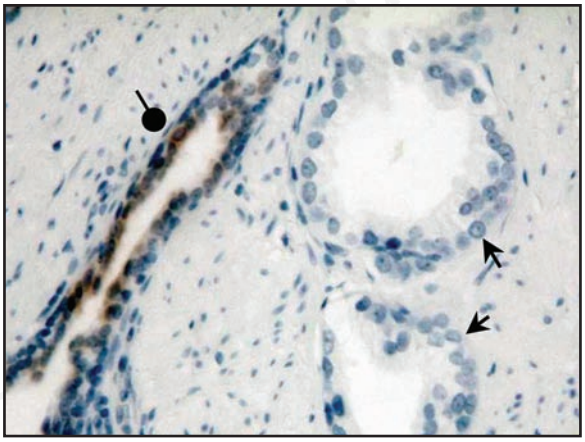

Figure 2. ASS expression in prostate cancer tissue by immunohistochemistry. ASS is readily expressed in benign prostate glands (round arrowhead) with heavy luminal staining by anti-ASS monoclonal antibody. In contrast, no ASS reactivity is detected in cancerous prostate glands (arrows).

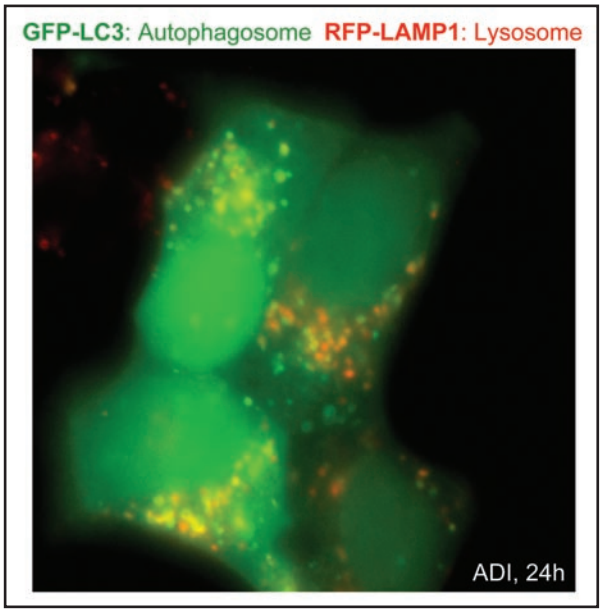

Figure 3. Autophagosome formation by ADI. CWR22R*v*1 cells overexpressing GFP-LC3 and RFP-LAMP-1 labeled proteins were treated with 0.3 μg/mL ADI for 24 hours. Individual autophagosomes (green), lysosomes (red), and the co-localization of both structures (yellow) are readily observed.

autophagy

volume 5 • issue 1 • 16 may 2009

LANDES BIOSCIENCE

Indexed in: Medline, PubMed and Sci Web of Science
www.landesbioscience.com/journals/autophagy